Modelling metrics for mine counter measure operations

B. Nguyen, PhD and R. Mirshak, PhD
Maritime Operational Research Team
DRDC - Center for Operational Research and Analysis

Defence Research and Development Canada

Scientific Report
DRDC-RDDC-2014-R58
August 2014

Modelling metrics for mine counter measure operations

B. Nguyen, PhD and R. Mirshak, PhD
Maritime Operational Research Team
DRDC - Center for Operational Research and Analysis

Defence Research and Development Canada

Scientific Report
DRDC-RDDC-2014-R58
August 2014

© Her Majesty the Queen in Right of Canada, as represented by the Minister of National Defence, 2014

© Sa Majesté la Reine (en droit du Canada), telle que représentée par le ministre de la Défense nationale, 2014

Abstract

In this scientific report, we present a methodology to determine the expected probabilities of detection of a target based on multiple looks at that target. We provide a sensitivity analysis of the probabilities of detection based on the number of looks, tactics and cross sections. Generally, the probability of detection improves significantly with the number of looks. Its value can vary substantially with the search and detection tactics as well as the cross section of a target. There are three tactics identified here where each look is independent of the others. The first tactic is a globally optimal tactic where the consecutive look angles are equidistant. The second tactic distributes the look angles randomly. The third tactic imposes the same angle for all look angles. In addition, we extract the guaranteed best angle of the broad side of a target from the first tactic. For each tactic, we propose an example of a corresponding search pattern. The methodology in this report can be implemented easily on any computational symbolic software; MathCad version 14 was used herein. We hope to make the search and detection community aware of the phenomenologies of multiple looks, and hope that the material presented will be incorporated into the mine search and detection tactics of the CAF.

Significance to defence and security

We provide a methodology to determine the expected probability of detection. This methodology accounts for the number of looks at a target, the tactics employed by the searcher and the cross section of that target. Generally, the probability of detection improves with the number of looks especially between the one look case and the two look case. The probabilities of detection for three search tactics are considered, and for a cylindrical target, are ranked in terms of effectiveness as follows:

1. A globally optimal tactic, where the headings for each of the passes are equally spaced;
2. A random-look tactic, where the heading for each pass is chosen randomly; and
3. A same-look tactic, where the search asset repeatedly passes over the object on the same heading.

In addition, for the globally optimal tactic, we calculate the maximum possible offset between the ideal heading (i.e., passing the target on broad side) and the best heading realized (i.e., the one that came closest to passing the target on the broad side).

The results presented in this report demonstrate the usefulness of multiple looks in search and detection operations and show quantitatively how the number of looks, the tactics, and the target cross section are combined in the calculation of the expected probability of detection. The findings can be used to improve the planning of search and detection missions prior to deployment.

Résumé

Dans le présent rapport scientifique, nous exposons une méthodologie pour déterminer les probabilités attendues de détection d'une cible en multivisée. Nous exposons une analyse de sensibilité des probabilités de détection fondées sur le nombre de visées, les tactiques et les sections efficaces radar . De façon générale, la probabilité de détection augmente de façon importante avec le nombre de visées. Sa valeur peut varier considérablement en fonction des tactiques de recherche et de détection et de la section efficace radar. Nous présentons ici trois tactiques dans lesquelles chaque visée est indépendante des autres. La première est une tactique optimale globale dans laquelle les angles de visée consécutifs sont équidistants. Dans la deuxième tactique, les angles de visée sont répartis aléatoirement. Quant à la troisième tactique, tous les angles de visée sont identiques. En outre, la première tactique nous permet de déduire le meilleur angle garanti du flanc d'une cible. Pour chaque tactique, nous proposons un exemple du circuit de recherche correspondant. La méthodologie présentée dans le rapport peut être mise en œuvre facilement à l'aide de n'importe quel logiciel de calcul symbolique; de notre côté, nous avons utilisé la version 14 de MathCad. Nous souhaitons sensibiliser la communauté de la recherche et de la détection aux phénomènes des visées multiples, et nous espérons que le matériel présenté sera intégré aux tactiques de recherche et de détection des mines des FAC.

Importance pour la défense et la sécurité

Nous présentons une méthodologie pour déterminer les probabilités attendues de détection . Cette méthodologie tient compte du nombre de visées en direction d'une cible, des tactiques employées par le chercheur et de la section efficace radar. En règle générale, la probabilité de détection augmente avec le nombre de visées, surtout entre un cas à une visée et un cas à deux visées. Les probabilités de détection de trois tactiques de recherche sont examinées; pour une cible cylindrique, ces tactiques sont classées d'après leur efficacité de la façon suivante :

1. 1. Une tactique optimale globale, dans laquelle les caps de chacun des passages sont équidistants;
2. 2. Une tactique à angles de visée aléatoires, dans laquelle le cap de chaque passage est déterminé au hasard;
3. 3. Une tactique à angles de visée identiques, dans laquelle l'instrument de recherche passe de façon répétitive au-dessus de l'objet en suivant le même cap.

De plus, dans le cas de la tactique optimale globale, nous avons calculé le décalage maximal possible entre le cap idéal (c.-à-d. celui qui passe sur le flanc de la cible) et le meilleur cap atteint (c.-à-d. celui qui est passé le plus près du flanc de la cible).

Les résultats compilés dans le présent rapport démontrent l'utilité des visées multiples dans les opérations de recherche et de détection et illustrent quantitativement comment le nombre de visées, les tactiques et la section efficace radar sont combinés dans le calcul de la probabilité attendue de détection . Les conclusions peuvent servir à améliorer la planification des missions de recherche et de détection avant un déploiement.

Table of contents

Abstract ……. i
Significance to defence and security i
Résumé ……. ii
Importance pour la défense et la sécurité ii
Table of contents iii
List of figures iv
List of tables v
Acknowledgements vi
1 Introduction 1
2 Justification 3
3 Problem statement 4
4 Imperfect detection as a function of range 8
5 A family of single look detection probability 14
6 Guaranteed broad side angle (GBSA) 18
7 Numerical results for a simplified model of mines 22
8 Ellipsoidal mine 36
9 Discussion 40
10 Conclusion 42
References 44
List of symbols/abbreviations/acronyms/initialisms 46

List of figures

Figure 1: Pen observed at different observation angles. 3
Figure 2: Cylindrical target observed at angle x. 4
Figure 3: Symmetries of the target. 5
Figure 4: Probability of not detecting a single target as a function of observation angle. 6
Figure 5: Radial symmetry for the optimal looks (two to five looks). 7
Figure 6: Symmetry. 19
Figure 7: Aspect angle as a function of target orientation for the two-look problem. 19
Figure 8: Aspect angle as a function of target orientation for the four-look problem. 21
Figure 9: Expected maximal probabilities of detection as a function of SLRDP for multiple looks. 24
Figure 10: Single look probability of no detection as a function of aspect angle for multiple cross sections. 25
Figure 11: Expected probabilities of detection as a function of SLRDP for multiple tactics based on one look. 26
Figure 12: Expected probabilities of detection as a function of SLRDP for multiple cross sections based on one look. 27
Figure 13: Expected probabilities of detection as a function of SLRDP for multiple tactics based on two looks. 28
Figure 14: Expected probabilities of detection as a function of SLRDP for multiple cross sections based on two look. 29
Figure 15: Expected probabilities of detection as a function of SLRDP for multiple tactics based on three looks. 30
Figure 16: Expected probabilities of detection as a function of SLRDP for multiple cross sections based on three looks. 31
Figure 17: Expected probabilities of detection as a function of SLRDP for multiple tactics based on four looks. 32
Figure 18: Expected probabilities of detection as a function of SLRDP for multiple cross sections based on four looks. 33
Figure 19: Expected probabilities of detection as a function of SLRDP for multiple tactics based on five looks. 34
Figure 20: Expected probabilities of detection as a function of SLRDP for multiple cross sections based on five looks. 35
Figure 21: A mine modelled as an ellipsoid. 36
Figure 22: Single look probabilities of no detection as a function of angle ν 38
Figure 23: Expected maximal probabilities of no detection as a function of SLRDP for multiple looks. 39

List of tables

Table 1: Examples considered. 23

Acknowledgements

We’d like to thank Alex Bourque for discussions on the guaranteed broad side look metric.

1 Introduction

In mine countermeasure operations, it is known that the detection performance improves when a target is observed many times at different aspect angles (Ref [1]). Similarly, classification algorithms (Refs [2][3][4]), and fixed sensor-arrays deployed for target localization and tracking (Refs [5][6][7][8][9]) benefit from multi-aspect observations. This fact is, however, often overlooked or not applied in practice. For example, the formula for the probability of detecting a target in a random search derived by Koopman is widely used yet it assumes no angular dependence (Ref [10]).

In a series of publications considering tactics for mine detection operations, Refs [11][12][13][14][15][16] examined the effectiveness of different strategies at detecting targets with mirror symmetry. In those studies, it was shown not only that multiple looks improve the probability of detecting such a target, but that in the globally optimal strategy that includes multiple looks, the angle between the looks are equidistant. That is, for n looks, the separation between any two consecutive looks is equal to π / n. This result was obtained under the following assumptions:

a. The single look detection probability takes on a specific, fixed form;

b. The Single Look Range Detection Probability (SLRDP) is 100%; and

c. The minimal single look angular detection probability is 0%.

In this TM, we demonstrate that the globally optimal tactic described above holds when these assumptions are relaxed. That is, we consider a general SLRDP, simulate the cross section through a class of single look detection probability functions and account for a non-zero minimal cross section corresponding to non-zero minimal single look angular detection probability.

Before we delve into the substance of this report, we will briefly summarize the context and the results that were obtained in Refs [11][12][13][14][15][16]. It is known that the detection performance improves when a target is observed many times at different aspect angles (Ref [1]) in mine counter measure operations. Similarly, classification algorithms (Refs [2][3][4]), and fixed sensor-arrays deployed for target localization and tracking (Refs [5][6][7][8][9]) benefit from multi-aspect observations. This fact is, however, often overlooked or not applied in practice. For example, the formula for the probability of detecting a target in a random search derived by Koopman is widely used yet it assumes no angular dependence (Ref [10]).

In Ref [12], search strategies that are associated with critical look angles of the overall probability of detecting a target observed at several different angles are identified. For example, a simple lawn mowing search pattern could be considered as a search strategy with one look. Out of the complete set of critical look angles, we determine the one that is globally maximal in the sense that the probability of detection is a global maximum. In principle, finding critical look angles (critical points in general) is a priori intractable as it is multi-dimensional in the sense that each observation is independent of one another and hence each observation angle must be considered as a separate dimension. What is more, the explicit expression for the overall probability of

detection can be extremely complicated even when the probability of detection for a single observation is simple and the number of observations few.

Fortunately, this problem can be solved using an elegant symmetry argument. Specifically, targets are assumed to exhibit rectangular symmetry. That is, the left hand side of a target is the mirror image of its right hand side, and the rear end is the mirror image of its front end. Many targets can be approximated with this class of symmetry including hull forms, mines and human bodies.

Using these assumptions, it was shown that observations evenly distributed on the half-circle as in Ref [9] corresponds to the globally maximal probability of detection. This constitutes a departure from the current literature on sensor geometry Refs [5][6][7][8][9] as our result is derived for cylinder like targets rather than for point targets.

The simplicity of the solution implies that no complicated calculations are required prior to a search as long as the target has the assumed approximate symmetry. This fact should improve the task of planning the path of mobile sensors, such as unmanned vehicles, to search for fixed targets, as well as of deploying a fixed sensor array to monitor traffic through choke points. We emphasize the fact that the globally optimal solution holds for all single look probability of detection function that obeys the mirror symmetry.

This TM derives analytical expressions for the expected probabilities of detection for a number of search strategies as well as the guaranteed best look angles corresponding to these search strategies. The TM also performs sensitivity analyses on these metrics. We present the material as follows. In Section 2, we provide the justification for the necessity of multiple looks. In Section 3, we define the modelling parameters. In Section 4 and Section 5, we derive close form solutions for the probabilities of detection for two classes of single look probability of detection. In Section 5, we analyze the guaranteed best look angle. In Section 7, we illustrate the sensitivities of the probabilities of detection based on the number of looks, tactics and cross sections for a simplified model of mines. In Section 8, we model a mine as an ellipsoid with realistic dimensions and demonstrate the influence of a non-zero minimal cross section. A discussion and a conclusion are given in Section 9 and Section 10 respectively.

2 Justification

In this Section, the qualitative dependence of the probability of detection as a function of angle is illustrated. A pen is put on a Christmas tree and pictures of the tree (including the pen) are taken as the tree is rotated by approximately 30 degrees each time.[1] This pen exhibits near rectangular symmetry and is approximately six inches in length. From Figure 1, it is difficult to identify the pen when angle is 60 degrees; even visually impossible when the angle is 90 degrees, but is easily identified when the angle is zero degree or 30 degrees.

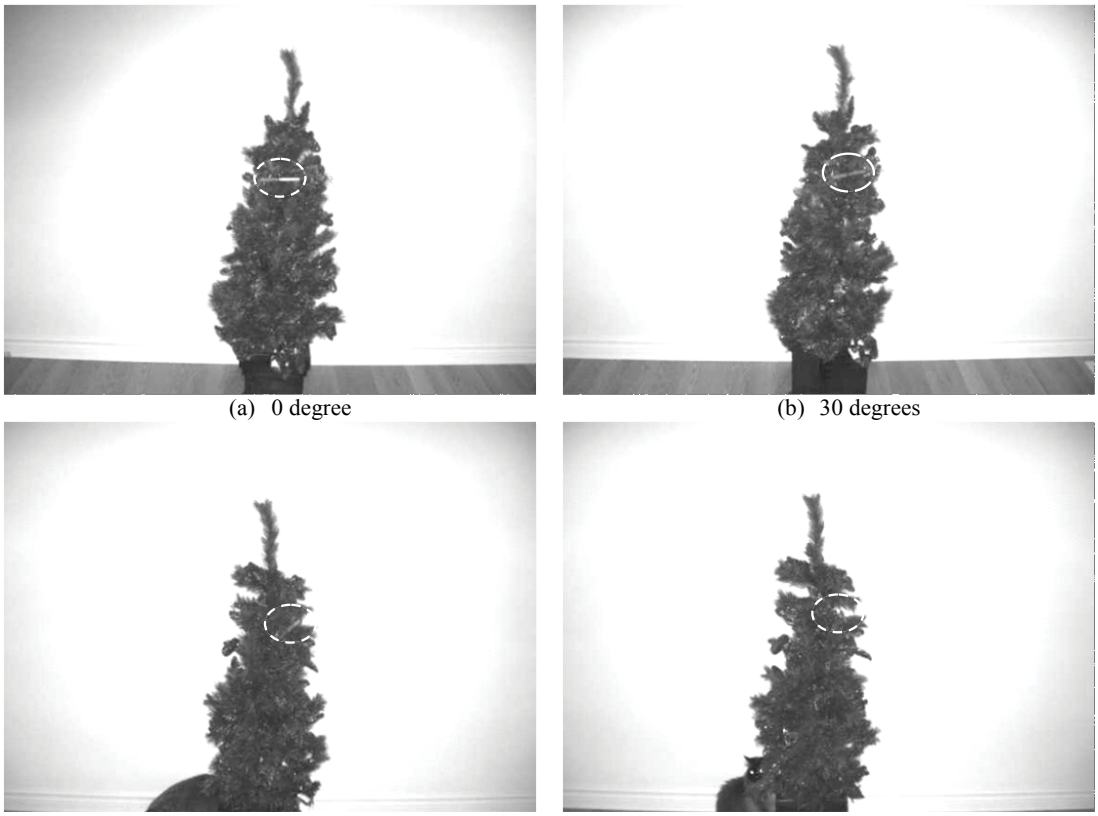

(a) 0 degree (b) 30 degrees

(c) 60 degrees (d) 90 degrees

Figure 1: *Pen observed at different observation angles.*

The experiment above shows how detection performance is affected by the observation angle. In addition, it highlights how the probability of detection improves with multiple observations at different angles. For example, if the pen is first observed at 60 degrees, then it is difficult to identify. However, if the pen is further observed at zero degree, then it is easily identified. Because the orientation of the target is not known a priori, it follows that making observations at multiple angles is a valid tactic to improve the probability of detection, Refs [1][2][3][4][5][6].

[1] The pen is approximately 15 cm in length. The tree is about 1 m in height. The distance between the camera and the tree is approximately 1.5 m. A cat is shown to give an idea of the scale. A Canon Power Shot A530 digital camera is used.

3 Problem statement

As shown in Section 2, the dependence of detection process on angle occurs often in search and detection operations. In addition, the effectiveness of such an operation also depends on the distance between the sensor and the target. It is reasonable to assume that the probability of detection as a function of range is constant i.e., at a fixed range the probability of detection at a particular angle is fixed, Ref [15].

As shown in Figure 2, the problem is modeled on a two-dimensional plane and the observation angle, x, is defined as the counter-clockwise angle measured in radian between the sensor beam and the short axis of a target. An observation angle of 0º corresponds to the observation of the long side of the target, while an observation angle of $\pi/2$ radians corresponds to the observation of the short side of the target. Targets considered will have approximate symmetries as shown in Figure 3. That is, they possess a reflection axis through their short axis (dashed line), and a rotation by 180º around the centre (dot-dashed line).[2] Human bodies, hull forms and mines have these types of symmetries.

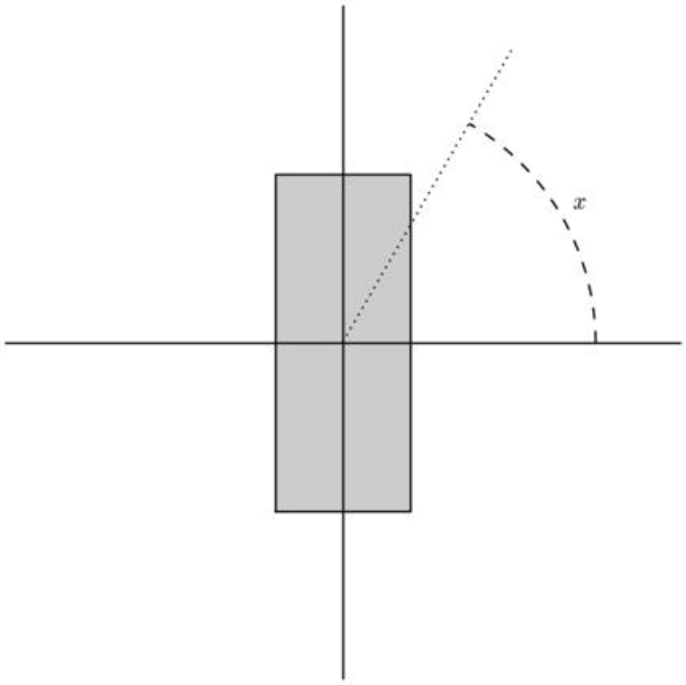

Figure 2: *Cylindrical target observed at angle* x.

[2] The composition of a reflection through the short axis followed by a rotation through the centre of the target is equivalent to a reflection through the long axis of the target (front-end/back-end mirror symmetry).

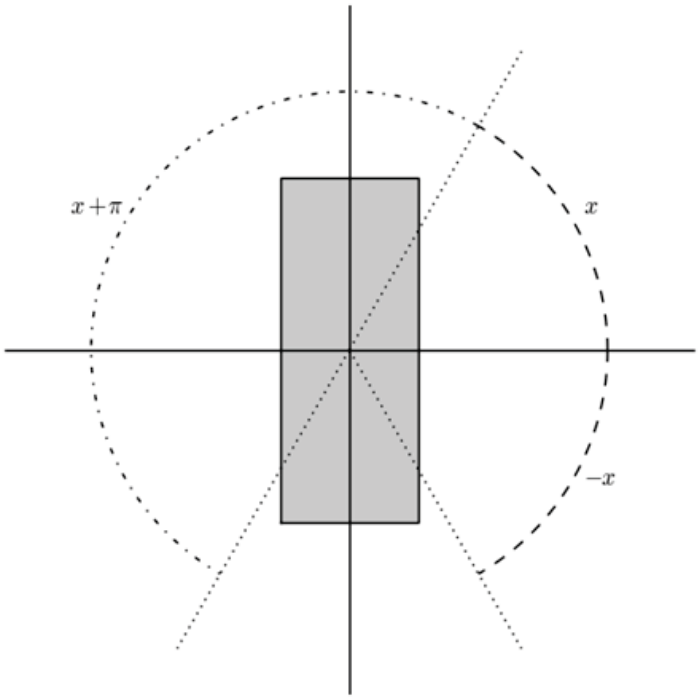

Figure 3: *Symmetries of the target.*

In what follows, the probability of no detection rather than the probability of detection is considered; one being the complement of the other. Define the single probability of no detection as the probability of not detecting a single target at angle x and denote this single-value real function as $g(x)$. Note that the single probability of no detection is even due to the reflection symmetry through the short axis of the target and periodic due to the rotation of 180º around the target's centre. Specifically,

$$g(x) = g(-x),$$

and

$$g(x) = g(x + \pi).$$

As an example consider $g(x) = \sin(x)^2$. From Figure 4, it is clear that it substantially increases if the observation angle differs from 0º, i.e., the single probability of not detecting the target depends significantly on the angle of observation.

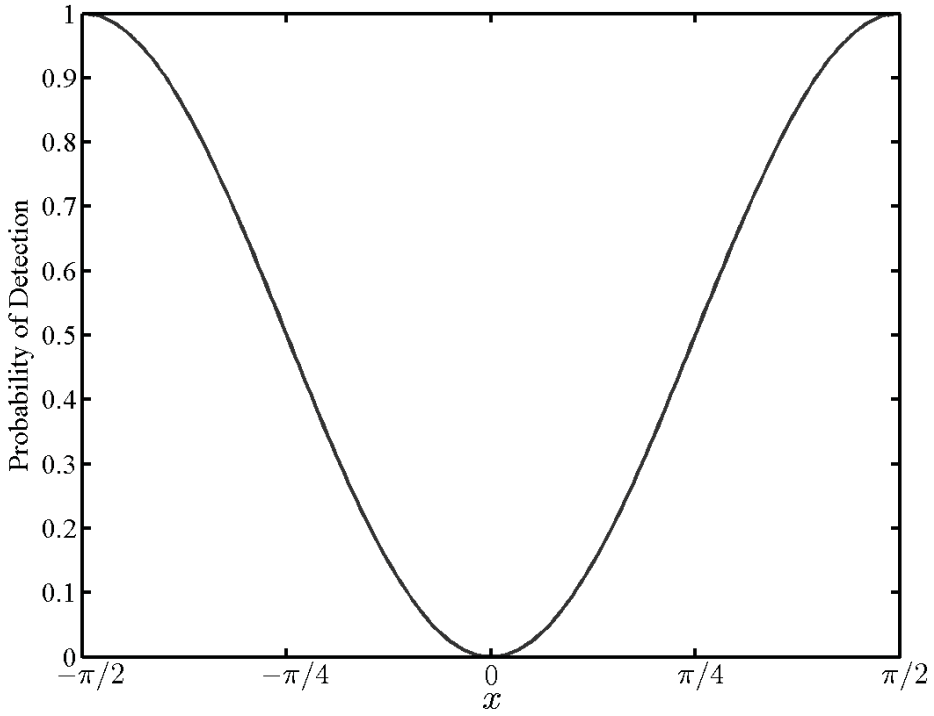

Figure 4: *Probability of not detecting a single target as a function of observation angle.*

Next, define the multiple probability of no detection as the probability of not detecting a single target after n observations. Let μ_i be the i-th angle at which the target is observed relative to x and $\vec{\mu} = (\mu_o, \dots, \mu_{n-1})$ be the vector of the n relative observation angles. Assume the multiple observation detection process is a Bernoulli process, i.e., all observations are independent. Then, the multi-observation probability of no detection is modeled as the product of single probabilities of no detection. In general, however, the exact value of x, i.e., the orientation of the target is unknown. To circumvent this problem, assume that the target's orientation is uniformly distributed and evaluate the average multiple probability of not detecting a single target. Denote this quantity by $G(\vec{\mu})$. Then,

$$G(\vec{\mu}) = \frac{1}{\pi}\int_{-\frac{\pi}{2}}^{\frac{\pi}{2}} dx g(x+\mu_0)g(x+\mu_1)\dots g(x+\mu_{n-1})\,. \tag{3.1}$$

The probability of detection can be written as:

$$P(\vec{\mu}) = 1 - G(\vec{\mu}) \tag{3.2}$$

The problem is then defined as finding search strategies that are critical values of $G(\vec{\mu})$. Below such a set of search strategy is identified. From it, a lower bound of the probability of no detection is also estimated.

For simplicity, the probability of no detection is taken to mean the average multiple look probability of no detection in the next sections. This is a key assumption.

It was found in Refs [11][12][13][14][15][16] that, for n looks, the optimal search strategies correspond to $\mu_i = i \cdot \mu$ with $i = 0,...,n-1$ where $\mu = \frac{m \cdot \pi}{n}$ where $m = 0,...,n$. The global maximum occurs when $m = 1$. Figure 5 displays the radial symmetry of the optimal looks.

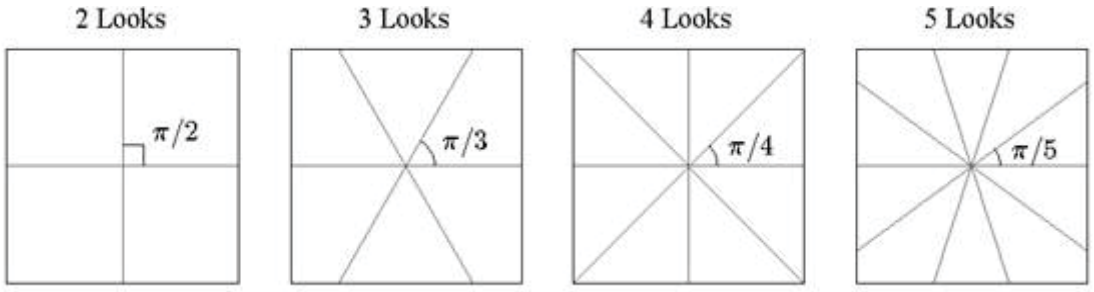

Figure 5: *Radial symmetry for the optimal looks (two to five looks).*

Note that as written Eqn (3.1) is not exactly correct as it assumes that each look is independent of one another. If a searcher observes a target with the same look (and the same range) then there is no information gain. If a searcher observes a target with a different look (and the same range) then there is information gain. Hence, the optimal tactic remains optimal when we consider correlation as long as $\mu = \pi / n$ is sufficiently large such that consecutive looks are independent. However, if a searcher repeats the same look then there is no improvement in the probability of detection. Though, technically, there may be some benefit if the multiple passes permit averaging and thus reducing the signal-to-noise ratio. We are assuming here, however, that the signal-to-noise ratio is high enough that it can be neglected.

4 Imperfect detection as a function of range

In this section, we assume that the single look probability of detection is equal to:

$$g(x) = 1 - P_r \cdot \sin(x)^2 \tag{4.1}$$

where P_r $(Q_r = 1 - P_r)$ is the probability of (no) detection based on range only and $0 \le P_r \le 1$. Technically, to be consistent with the definition of $g(x)$ in the previous section, the single look probability of detection should be equal to:

$$g(x) = 1 - P_r \cdot \cos(x)^2 \tag{4.2}$$

However, since $g(x)$ is periodic with periods equal to π, there is no difference in $G(\bar{\mu})$ whether we use Eqn (4.1) or Eqn (4.2). That is, we can shift the variable of integration x by $\pi/2$ in Eqn (3.1) without affecting the value of $G(\bar{\mu})$. For convenience, we adopt Eqn (4.1). Note that,

$$g(x) = 1 - P_r \cdot \sin(x)^2 = Q_r + P_r \cdot \cos(x)^2 = Q + P \cdot \cos(x)^2 \tag{4.3}$$

where we suppress the index r to lighten the notation and observe that $P + Q = 1$.

Lemma 4A. The globally maximum probability of detection assuming the single look probability of no detection in Eqn (4.3) is equal to:

$$\begin{aligned} P_e(1,n) &= 1 - \frac{1}{\pi} \cdot \int_0^{\pi} dx \cdot g(x) \cdot g\left(x + \frac{\pi}{n}\right) \cdot \ldots \cdot g\left(x + (n-1) \cdot \frac{\pi}{n}\right) \\ &= 1 - 2 \cdot \left(\frac{P}{4}\right)^n \cdot \cosh(n \cdot \phi) \end{aligned} \tag{4.4}$$

where

$$\cosh(\phi) = 1 + 2 \cdot \frac{Q}{P} \tag{4.5}$$

Proof of Lemma 4A. Consider the integrand of Eqn (4.4):

$$
\begin{aligned}
I_n(x) &= \prod_{i=0}^{n-1} g\left(x + i\cdot\frac{\pi}{n}\right) = \prod_{i=0}^{n-1}\left[Q + P\cdot\cos\left(x + i\cdot\frac{\pi}{n}\right)^2\right] \\
&= \prod_{i=0}^{n-1}\left[Q + \frac{P}{2}\cdot\left(1 + \cos\left(2x + i\cdot\frac{2\pi}{n}\right)\right)\right] \\
&= \prod_{i=0}^{n-1}\left[Q + \frac{P}{2} + \frac{P}{2}\cdot\cos\left(2x + i\cdot\frac{2\pi}{n}\right)\right] \\
&= \left(\frac{P}{2}\right)^n \cdot \prod_{i=0}^{n-1}\left[\frac{Q + \frac{P}{2}}{\frac{P}{2}} + \cos\left(2x + i\cdot\frac{2\pi}{n}\right)\right]
\end{aligned}
\tag{4.6}
$$

Define

$$\cosh(\phi) = 1 + 2\cdot\frac{Q}{P}$$

$$2\cdot x = 2\cdot x' + \pi$$

We can rewrite Eqn (4.6) as:

$$I_n(x') = \left(\frac{P}{2}\right)^n \cdot \prod_{i=0}^{n-1}\left[\cosh(\phi) - \cos\left(2\cdot x' + i\cdot\frac{2\pi}{n}\right)\right]$$

Using Ref [17], we get:

$$
\begin{aligned}
I_n(x) &= 2\cdot\left(\frac{P}{4}\right)^n \cdot\left(\cosh(n\cdot\phi) - \cos(2\cdot n\cdot x - n\cdot\pi)\right) \\
&= 2\cdot\left(\frac{P}{4}\right)^n \cdot\left(\cosh(n\cdot\phi) + (-)^{n+1}\cos(2\cdot n\cdot x)\right)
\end{aligned}
$$

Integrating $I_n(x)$ over x:

$$
\begin{aligned}
\frac{1}{\pi}\cdot\int_0^{\pi} dx\cdot I_n(x) &= \frac{1}{\pi}\cdot\int_0^{\pi} dx\cdot 2\cdot\left(\frac{P}{4}\right)^n \cdot\left(\cosh(n\cdot\phi) + (-)^{n+1}\cos(2\cdot n\cdot x)\right) \\
&= 2\cdot\left(\frac{P}{4}\right)^n \cdot\cosh(n\cdot\phi)
\end{aligned}
$$

Since

$$\frac{1}{\pi}\cdot\int_0^{\pi} dx\cdot\cos\left(2\cdot n\cdot x\right)=\delta_{0,n}=0$$

as $n\geq 1$. Hence the globally maximal detection probability is equal to:

$$P_e\left(1,n\right)=1-2\cdot\left(\frac{P}{4}\right)^n\cdot\cosh\left(n\cdot\phi\right)$$

We could make use of Eqn (4.5) to rewrite the above as:

$$\begin{aligned}P_e\left(1,n\right)&=1-\left(\frac{P}{4}\right)^n\cdot\left[\left(\cosh\left(\phi\right)+\sinh\left(\phi\right)\right)^n+\left(\cosh\left(\phi\right)-\sinh\left(\phi\right)\right)^n\right]\\&=1-\left(\frac{P}{4}\right)^n\cdot\left[\left(1+2\cdot\frac{Q}{P}+2\cdot\sqrt{\frac{Q}{P}\cdot\left(1+\frac{Q}{P}\right)}\right)^n+\left(1+2\cdot\frac{Q}{P}-2\cdot\sqrt{\frac{Q}{P}\cdot\left(1+\frac{Q}{P}\right)}\right)^n\right]\end{aligned}$$

QED (Quod Erat Demonstrandum). Below, we provide a formula for the probability of detection when m can be different from one.

Lemma 4B. The optimal probability of detection assuming the single look probability of no detection in Eqn (4.3) is equal to:

$$P_e\left(m,n\right)=1-2^p\cdot\left(\frac{P}{4}\right)^n\cdot\sum_{k=0}^{p}\binom{p}{k}\cdot\cosh\left(r\cdot\phi\right)^{p-k}\cdot\frac{\left(1+\left(-1\right)^k\right)}{2}\cdot\frac{k!}{\left(2^k\cdot\Gamma\left(k/2+1\right)^2\right)}\qquad(4.7)$$

where

$$\cosh\left(\phi\right)=1+2\cdot\frac{Q}{P}\qquad(4.8)$$

$$\mu=\frac{m\cdot\pi}{n}$$

and

$$m = p \cdot q$$
$$n = p \cdot r$$
$$p = \gcd(m, n)$$

For clarity, we note that the integer r as defined above is not the same as the label r associated with P_r. The former represents n / p while the latter represents range as in the probability of detection based on range.

Proof of Lemma 4B. Consider the integrand of Eqn (3.1), using Ref [12]:

$$I_{m,n}(x) = \prod_{i=0}^{n-1} g\left(x + i \cdot \frac{m \cdot \pi}{n}\right) = \left[\prod_{i=0}^{r-1} g\left(x + i \cdot \frac{m \cdot \pi}{n}\right)\right]^p$$
$$= \left[\prod_{i=0}^{r-1} \left\{Q + P \cdot \cos\left(x + i \cdot \frac{m \cdot \pi}{n}\right)^2\right\}\right]^p$$
$$= \left[\prod_{i=0}^{r-1} \left\{Q + P \cdot \cos\left(x + i \cdot \frac{q \cdot \pi}{r}\right)^2\right\}\right]^p$$
$$= \left[\prod_{i=0}^{r-1} \left\{Q + \frac{P}{2} \cdot \left(1 + \cos\left(2 \cdot x + i \cdot \frac{q \cdot 2 \cdot \pi}{r}\right)\right)\right\}\right]^p$$
$$= \left[\prod_{i=0}^{r-1} \left\{Q + \frac{P}{2} \cdot \left(1 + \cos\left(2 \cdot x + i \cdot \frac{2 \cdot \pi}{r}\right)\right)\right\}\right]^p$$
$$= \left(\frac{P}{2}\right)^n \cdot \left[\prod_{i=0}^{r-1} \left\{1 + 2 \cdot \frac{Q}{P} + \cos\left(2 \cdot x + i \cdot \frac{2 \cdot \pi}{r}\right)\right\}\right]^p$$

Use again Ref [17]:

$$\cosh(\phi) = 1 + 2 \cdot \frac{Q}{P}$$

$$2 \cdot x = 2 \cdot x' + \pi$$

$$I_{m,n}(x)=\left(\frac{P}{2}\right)^n\cdot\left[\prod_{i=0}^{r-1}\left\{\cosh(\phi)+\cos\left(2\cdot x'+i\cdot\frac{2\cdot\pi}{r}\right)\right\}\right]^p$$

$$=\left(\frac{P}{2}\right)^n\cdot\left(\frac{1}{2^{p\cdot(r-1)}}\right)\cdot\left[\cosh(r\cdot\phi)-\cos(2\cdot r\cdot x-r\cdot\pi)\right]^p$$

$$=2^p\cdot\left(\frac{P}{4}\right)^n\cdot\left[\cosh(r\cdot\phi)+(-)^{r+1}\cos(2\cdot r\cdot x)\right]^p$$

$$=2^p\cdot\left(\frac{P}{4}\right)^n\cdot\sum_{k=0}^{p}\binom{p}{k}\cdot(-)^{k\cdot(r+1)}\cdot\cos(2\cdot r\cdot x)^k\cdot\cosh(r\cdot\phi)^{p-k}$$

We observe that for $r\geq 1$:

$$\int_0^{\pi}dx\cdot\frac{\cos(2\cdot r\cdot x)^k}{\pi}=\begin{cases}\dfrac{k!}{2^k\cdot((k/2)!)^2} & k\ even\\ 0 & k\ odd\end{cases}$$

$$\int_0^{\pi}\frac{dx}{\pi}\cdot I_{m,n}(x)=2^p\cdot\left(\frac{P}{4}\right)^n\cdot\sum_{k=0}^{p}\binom{p}{k}\cdot(-)^{k\cdot(r+1)}\cdot\cosh(r\cdot\phi)^{p-k}\cdot\int_0^{\pi}\frac{dx}{\pi}\cdot\cos(2\cdot r\cdot x)^k$$

$$=2^p\cdot\left(\frac{P}{4}\right)^n\cdot\sum_{k=0}^{p}\binom{p}{k}\cdot(-)^{k\cdot(r+1)}\cdot\cosh(r\cdot\phi)^{p-k}\cdot\frac{\left(1+(-1)^k\right)}{2}\cdot\frac{k!}{\left(2^k\cdot\Gamma(k/2+1)^2\right)}$$

Hence

$$P_e(m,n)=1-2^p\cdot\left(\frac{P}{4}\right)^n\cdot\sum_{k=0}^{p}\binom{p}{k}\cdot\cosh(r\cdot\phi)^{p-k}\cdot\frac{\left(1+(-1)^k\right)}{2}\cdot\frac{k!}{\left(2^k\cdot\Gamma(k/2+1)^2\right)}$$

If $p=1=(m,n)$ then the only surviving term is $k=0$ and $r=n/p=n$, we get back the result of Lemma 4A. That is,

$$P_e(1,n)=1-2\cdot\left(\frac{P}{4}\right)^n\cdot\cosh(n\cdot\phi)$$

QED.

Lemma 4C. In deriving Lemmas 4A and 4B, we stumble on a few identities that are not trivial. We list them below without proof in case they may be useful in another type of derivation.

$$I_n(x) = \prod_{i=0}^{n-1} g\left(x + i \cdot \frac{\pi}{n}\right) = \prod_{i=0}^{n-1}\left[Q + P \cdot \cos\left(x + i \cdot \frac{\pi}{n}\right)^2\right]$$

$$= \prod_{i=0}^{n-1}\left[Q + P \cdot \cos\left(i \cdot \frac{\pi}{n}\right)^2\right] + \frac{P^n}{4^{n-1}} \cdot \sin\left(n\left(x + \frac{\pi}{2}\right)\right)^2 - \frac{P^n}{4^{n-1}} \cdot \sin\left(n \cdot \frac{\pi}{2}\right)^2$$

$$P_e(1,n) = \prod_{i=0}^{n-1}\left[Q + P \cdot \cos\left(i \cdot \frac{\pi}{n}\right)^2\right] + (-)^n \cdot \frac{2 \cdot P^n}{4^n} = 1 - 2 \cdot \left(\frac{P}{4}\right)^n \cdot \cosh(n \cdot \phi)$$

.

One could appreciate the non trivial nature of the equivalence of the two expressions above.

5 A family of single look detection probability

In this section, we consider $g(x) = |\sin(x)|^a$ where $a \geq 0$ is a parameter that adjusts to the shape of the target.

Lemma 5A. The optimal probability of detection is given by:

$$P_e(m,n) = 1 - \frac{1}{\sqrt{\pi} \cdot 2^{a \cdot (n-p)}} \cdot \frac{\Gamma\left(\frac{1}{2} \cdot (1 + a \cdot p)\right)}{\Gamma\left(\frac{a}{2} \cdot p + 1\right)}$$

where

$$\mu = \frac{m \cdot \pi}{n}$$

and

$$m = p \cdot q$$
$$n = p \cdot r$$
$$p = \gcd(m,n)$$

Proof of Lemma 5A. Consider the integrand of Eqn (3.1), using Ref [12]:

$$I_{m,n}(x) = \prod_{i=0}^{n-1} g\left(x + i \cdot \frac{m \cdot \pi}{n}\right) = \left[\prod_{i=0}^{r-1} g\left(x + i \cdot \frac{m \cdot \pi}{n}\right)\right]^p$$
$$= \left[\prod_{i=0}^{r-1} \left\{\sin\left(x + i \cdot \frac{m \cdot \pi}{n}\right)^{2 \cdot \frac{a}{2}}\right\}\right]^p \tag{4.9}$$

Using the identity, Ref [18]:

$$\sin(n \cdot x) = 2^{n-1} \cdot \prod_{k=0}^{n-1} \sin\left(x + \frac{k \cdot \pi}{n}\right)$$

We get:

$$I_{m,n} = \frac{1}{\pi} \cdot \prod_{k=1}^{p} \frac{\sin\left(r \cdot x\right)^{2 \cdot a'}}{4^{a' \cdot (r-1)}}$$

where $a' = a / 2$.

Substituting the above expression into Eqn (3.2), we obtain:

$$\begin{aligned} P_e\left(m,n\right) &= 1 - \frac{1}{\pi} \cdot \int_{-\pi/2}^{\pi/2} dx \cdot \prod_{k=1}^{p} \frac{\sin\left(r \cdot x\right)^{2 \cdot a'}}{4^{a' \cdot (r-1)}} \\ &= 1 - \frac{2}{\pi \cdot 4^{a' \cdot p \cdot (r-1)}} \cdot \int_{-\pi/2}^{\pi/2} dx \cdot \sin\left(x\right)^{2 \cdot a' \cdot p} \\ &= 1 - \frac{1}{\pi \cdot 4^{a' \cdot p \cdot (r-1)}} \cdot B\left(a' \cdot p + \frac{1}{2}, \frac{1}{2}\right) \\ &= 1 - \frac{1}{\pi \cdot 2^{a \cdot p \cdot (r-1)}} \cdot \frac{\Gamma\left(\frac{1}{2} \cdot \left(1 + a \cdot p\right)\right) \cdot \Gamma\left(\frac{1}{2}\right)}{\Gamma\left(\frac{a}{2} \cdot p + 1\right)} \\ &= 1 - \frac{1}{\sqrt{\pi} \cdot 2^{a \cdot (n-p)}} \cdot \frac{\Gamma\left(\frac{1}{2} \cdot \left(1 + a \cdot p\right)\right)}{\Gamma\left(\frac{a}{2} \cdot p + 1\right)} \end{aligned}$$

where $B\left(.,.\right)$ is the Beta function and Γ is the Gamma function. Note that:

$$\Gamma\left(p + \frac{1}{2}\right) = \frac{\sqrt{\pi} \cdot \left(2 \cdot p - 1\right)!!}{2^p}$$

If we let $a \to 2$ then

$$\lim_{a \to 2} P_e\left(m,n\right) = 1 - \frac{2^p \cdot \left(2 \cdot p - 1\right)!!}{4^n \cdot p!}$$

which is the result obtained in Ref [12]. Due to the global optimality of $P_e\left(1,n\right)$, we obtain the following inequality:

$$1 \geq \frac{1}{\sqrt{\pi} \cdot 2^{a \cdot (n-p)}} \cdot \frac{\Gamma\left(\frac{1}{2} \cdot (1 + a \cdot p)\right)}{\Gamma\left(\frac{a}{2} \cdot p + 1\right)} \geq \frac{1}{\sqrt{\pi} \cdot 2^{a \cdot (n-1)}} \cdot \frac{\Gamma\left(\frac{1}{2} \cdot (1 + a)\right)}{\Gamma\left(\frac{a}{2} + 1\right)}$$

or

$$2^{a \cdot (p-1)} \cdot \frac{\Gamma\left(\frac{1}{2} \cdot (1 + a \cdot p)\right)}{\Gamma\left(\frac{a}{2} \cdot p + 1\right)} \geq \frac{\Gamma\left(\frac{1}{2} \cdot (1 + a)\right)}{\Gamma\left(\frac{a}{2} + 1\right)}$$

where $p = \gcd(m, n)$. QED.

Lemma 5B. If the range detection performance is not perfect then the optimal probabilities of detection for n looks can be written as:

$$P_e(m, n) = 1 - \frac{1}{\pi} \cdot \int_{-\pi/2}^{\pi/2} dx \cdot \left[\prod_{i=0}^{r-1} \left\{ Q + P \cdot \left| \sin(x + i \cdot \mu) \right|^a \right\} \right]^p \tag{4.10}$$

where

$$\mu = \frac{m \cdot \pi}{n}$$

and

$$m = p \cdot q$$
$$n = p \cdot r$$
$$p = \gcd(m, n)$$

Proof of Lemma 5B. Substituting $g(x) = 1 - P \cdot \left[1 - \left| \sin(x) \right|^a \right] = Q + P \cdot \left| \sin(x) \right|^a$ into Eqn (4.9) and using Eqns (3.1) &(3.2), we obtain Eqn (4.10). The proof of Lemma 5B is now complete. QED.

Lemma 5C. If the range detection performance is not perfect and the look angles are uniformly distributed then the expected probability of detection can be written as:

$$P_e(n) = 1 - \left\{ Q + \frac{2^a}{\pi} \cdot P \cdot B\left(\frac{1+a}{2}, \frac{1+a}{2} \right) \right\}^n \tag{4.11}$$

Proof of Lemma 5C. As in the proof of Lemma 5B, the single look density distribution can be expressed as:

$$g(x+\mu) = Q + P \cdot \left| \sin(x+\mu) \right|^a$$

where μ is the look angle. If μ is uniformly distributed then its density distribution is $1/\pi$. Substituting the above equation into Eqn (3.2), we get:

$$\begin{aligned} P_e(n) &= 1 - \int_{-\pi/2}^{\pi/2} \frac{dx}{\pi} \int_{-\pi/2}^{\pi/2} \frac{d\mu_0}{\pi} \cdots \int_{-\pi/2}^{\pi/2} \frac{d\mu_{n-1}}{\pi} \cdot \prod_{i=0}^{n-1} \left\{ Q + P \cdot \left| \sin(x+\mu_i) \right|^a \right\} \\ &= 1 - \int_{-\pi/2}^{\pi/2} \frac{dx}{\pi} \cdot \prod_{i=0}^{n-1} \left[\int_{-\pi/2}^{\pi/2} \frac{d\mu_i}{\pi} \cdot \left\{ Q + P \cdot \left| \sin(x+\mu_i) \right|^a \right\} \right] \end{aligned} \tag{4.12}$$

Since $\sin(x)$ is a periodic function, we infer that:

$$\begin{aligned} \int_{-\pi/2}^{\pi/2} \frac{d\mu_i}{\pi} \cdot \left\{ Q + P \cdot \left| \sin(x+\mu_i) \right|^a \right\} &= \int_{-\pi/2}^{\pi/2} \frac{d\mu_i}{\pi} \cdot \left\{ Q + P \cdot \left| \sin(\mu_i) \right|^a \right\} \\ &= Q + P \cdot \frac{2^a}{\pi} \cdot B\left(\frac{1+a}{2}, \frac{1+a}{2} \right) \end{aligned}$$

where the last equality comes from Ref [19] and $B(.,.)$ is the beta function. Using the above equation and Eqn (4.12), we get:

$$P_e(n) = 1 - \left\{ Q + \frac{2^a}{\pi} \cdot P \cdot B\left(\frac{1+a}{2}, \frac{1+a}{2} \right) \right\}^n \tag{4.13}$$

This concludes Lemma 5C. QED.

6 Guaranteed Broad Side Angle (GBSA)

The idea behind the multiple look concept is that by observing a target from multiple angles we improve the chance of observing that target along its broad side. The best look angle is of course $\pi/2$ which corresponds to the geometry where the sensor beam is perpendicular to the broad side of a target. In this section, we determine the guaranteed broad side angle (GBSA) in the globally optimal tactic. That is, given n looks μ_i where $i = 0,...,n-1$ such that $\mu_i = i \cdot \mu$ and $\mu = \frac{\pi}{n}$, we derive the smallest angle of observation of the broad side of a target assuming that the orientation of that target is uniformly distributed. This smallest angle is defined as the GBSA i.e., the searcher will always view the broad side of a target at GBSA or better. To motivate the analysis, we examine the case of two looks below.

Example 6A. Let the orientation of a target be θ measured counter clockwise from the horizontal axis. For $n = 2$, we have $\bar{\mu} = \left(0, \frac{\pi}{2}\right)$. As shown in Figure 7, the two observation angles are simply:

$$\nu_0 = \frac{\pi}{2} - \theta$$
$$\nu_1 = \theta$$

The best angle of observation is $\nu_{\max} = \max(\nu_0, \nu_1) = \max\left(\frac{\pi}{2} - \theta, \theta\right)$. The worst of the best case is obtained by minimizing $\nu_{\max}$ over all possible θ i.e., $\hat{\nu} = \min_{0 \le \theta \le \pi/2} \nu_{\max} = \min_{0 \le \theta \le \pi/2} \max(\nu_0, \nu_1)$. Technically, we need to consider $\theta \in [0, 2 \cdot \pi]$. However, due to the symmetry that we assume for a target, it is sufficient to examine $\theta \in [0, \pi/2]$ as shown in Figure 6 where the two observation angles are along the horizontal axis and the vertical axis respectively. In Figure 7, we plot out ν_0 and ν_1 as a function of θ. It is easily seen that lowest of $\nu_{\max}$ occurs at $\theta = \frac{\pi}{4}$. Hence,

$$\hat{\nu} = \min_{0 \le \theta \le \pi/2} \nu_{\max} = m\,\mathrm{ax}\left(\frac{\pi}{2} - \frac{\pi}{4}, \frac{\pi}{4}\right) = \frac{\pi}{4}$$

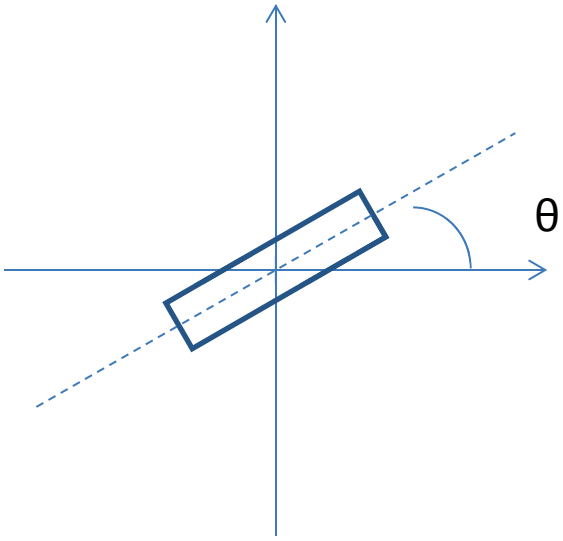

Figure 6: *Symmetry.*

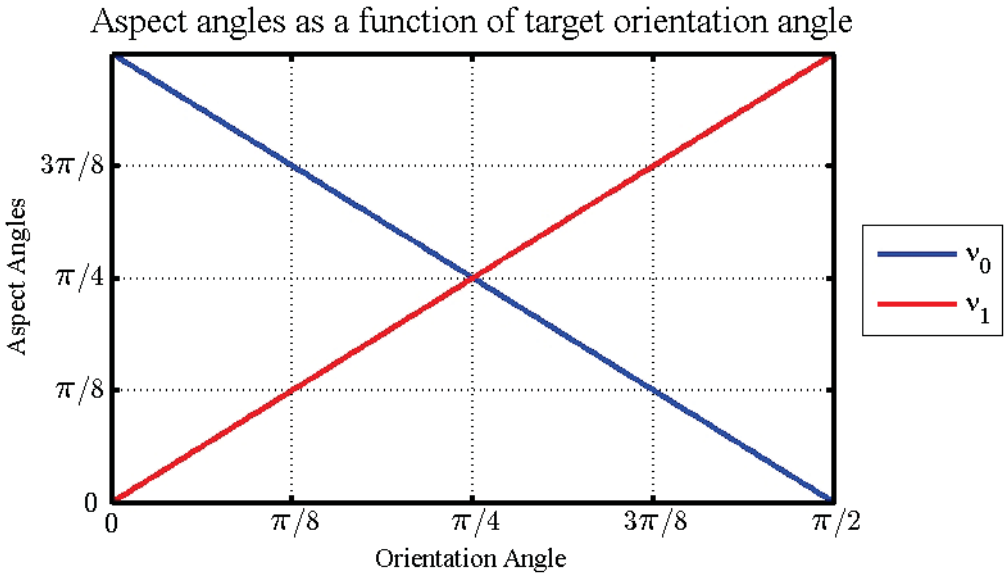

Figure 7: *Aspect angle as a function of target orientation for the two-look problem.*

Lemma 6A. Given the globally optimal tactic as stated above, it is guaranteed that a target will be observed in the worst case at the angle:

$$\hat{\nu} = \min_{(0 \le \theta \le \pi/2)} \max_{(i=0,\ldots,n-1)} \left(\nu_i(\theta)\right) = \frac{\pi}{2} \cdot \left(1 - \frac{1}{n}\right)$$

Proof of Lemma 6A. Given a look angle φ on a target with an orientation angle θ, the aspect angle can be expressed as:

$$\nu_{\varphi}(\theta) = \begin{cases} \frac{\pi}{2} - (\theta - \varphi) & if\ \varphi \le \theta \\ \frac{\pi}{2} + (\theta - \varphi) & if\ \varphi > \theta \end{cases}$$

The globally optimal tactic dictates that $\varphi = \mu_i$ where $\mu_i = i \cdot \mu$ where $i = 0, ..., n-1$ and $\mu = \frac{\pi}{n}$. When we plot out $\nu_i(\theta) = \nu_{\varphi=\mu_i}(\theta)$ such as Figure 8, there is an emerging pattern which indicates that $\hat{\nu}$ occurs when $\nu_0(\hat{\theta}) = \nu_1(\hat{\theta})$. This implies that:

$$\frac{\pi}{2} - \hat{\theta} = \frac{\pi}{2} - \left(\frac{\pi}{n} - \hat{\theta}\right)$$

$$\hat{\theta} = \frac{\pi}{2 \cdot n}$$

Hence,

$$\hat{\nu} = \frac{\pi}{2} - \hat{\theta} = \frac{\pi}{2} \cdot \left(1 - \frac{1}{n}\right)$$

QED.

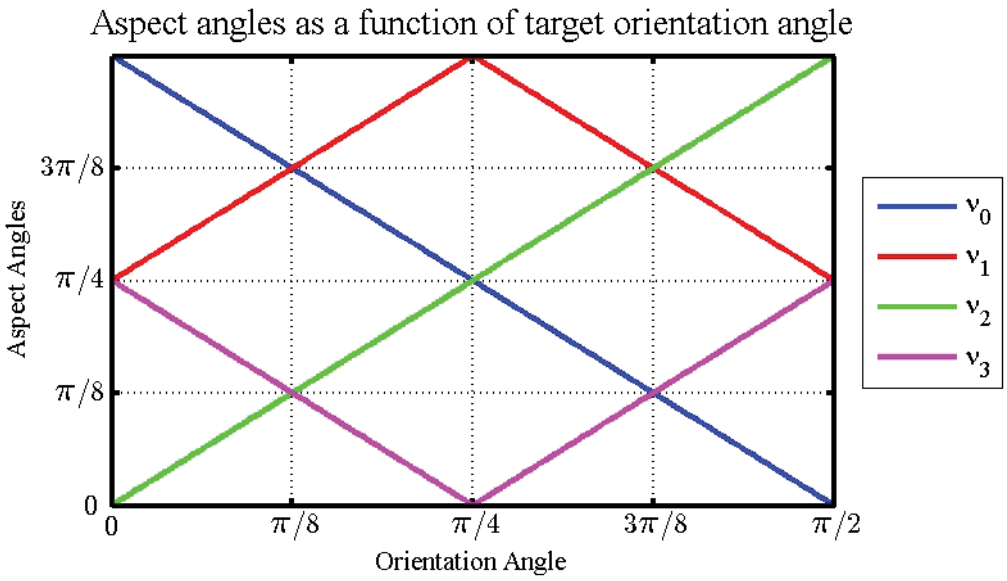

Figure 8: *Aspect angle as a function of target orientation for the four-look problem.*

7 Numerical results for a simplified model of mines

In this section, we provide examples that illustrate the sensitivity of the expected probabilities of detection from the modelling features: cross section of the target, single look probability of detection based on range, number of looks and tactics.

In the examples below, we provide expected probabilities of detection for three tactics:

i. "Equidistant Looks (EL)" indicates the globally maximal tactic is used as derived in Ref [16]. That is, the ith look angle $\mu_i = i \cdot \frac{\pi}{n}$ where $i = 0,...,n-1$ with n representing the total number of looks; "Guaranteed Broad Side Look (GBSL)" is an additional metric of the EL tactic which indicates that the searcher is guaranteed to observe a target at GBSA or better when he employs the EL looks. From Lemma 6A, $GBSA = \frac{\pi}{2} \cdot \left(1 - \frac{1}{n}\right)$.

ii. "Random Looks (RL)" indicates the look angle is uniformly random as derived in Lemma 5C. That is, the ith look angle μ_i is drawn randomly from the interval $[0, \pi]$.

iii. "Same Looks (SL)" indicates that the target is observed at the same angle possibly many times as derived in Ref [16]. That is, the i^{th} look angle is a constant c for all i $\mu_i = c$.

The examples considered are summarized in Table 1.

Table 1: *Examples considered.*

Example	Description
7A	Effect of one to five looks on expected maximal detection probability assuming EL tactic.
7B	Effect of cross-section on single look probability of no detection.
7C	Effect of Tactics i to iv on expected probability of detection assuming one look only.
7D	Effect of cross section on expected maximal probability of detection assuming one look.
7E	Effect of tactics on expected probability of detection assuming two looks.
7F	Effect of cross section on expected maximal probability of detection assuming two looks.
7G	Effect of tactics on expected probability of detection assuming three looks.
7H	Effect of cross section on expected maximal probability of detection assuming three looks.
7I	Effect of tactics on expected probability of detection assuming four looks.
7J	Effect of cross section on expected maximal probability of detection assuming four looks.
7K	Effect of tactics on expected probability of detection assuming five looks.
7L	Effect of cross section on expected maximal probability of detection assuming five looks.

Example 7A. Effects of multiple looks. In Figure 9, we plot the maximal probabilities of detection as a function of SLRDP(P) for up to five looks. The overall single look probability of detection is assumed to be $g(x)=(1-P)+P\cdot(\sin(x))^2$. The aimed probability threshold is set at 0.95. It is shown that with three looks or more, we can achieve this threshold. The requirement on P to meet this threshold becomes less stringent as the number of looks increases. For instance, with five looks $P\geq 0.8$ while with three looks $P\geq 0.97$. Generally, the maximal probabilities of detection increases with the number of looks. The most significant increase occurs when we go from one look to two looks. Note that, the curves shown in Figure 9 assume the searcher employs the EL tactic that was derived in Ref [16].

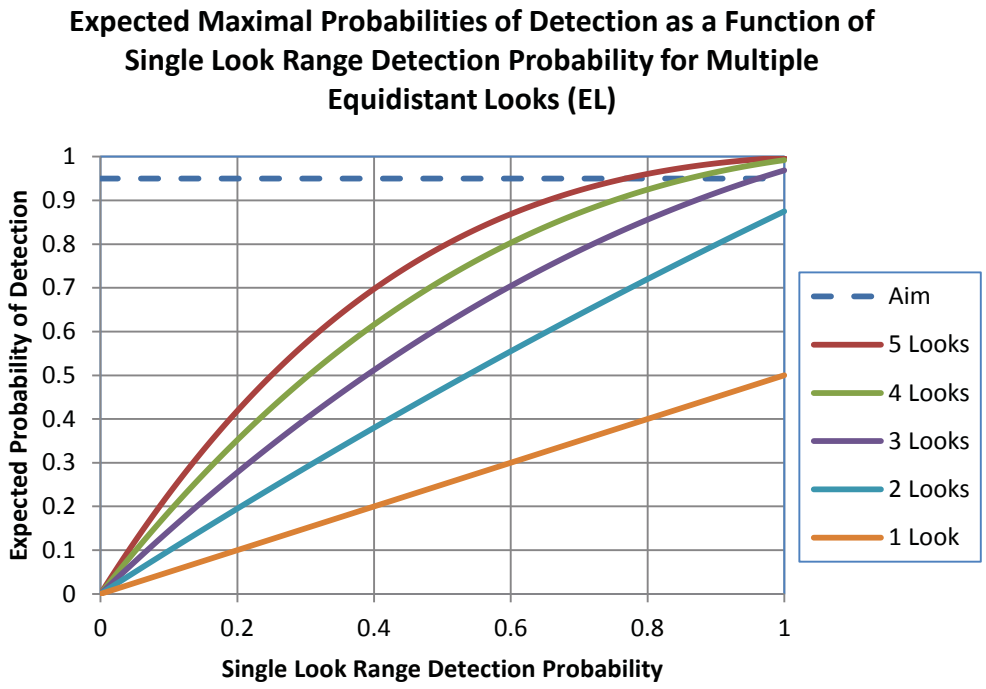

Figure 9: *Expected maximal probabilities of detection as a function of SLRDP for multiple looks.*

Example 7B. Effects of cross sections. In Figure 10, we plot the single look probability of no detection as a function of aspect angle for multiple cross sections. That is, $g(x) = (1-P) + P \cdot |\sin(x)|^a$ where $P = 1$. We simulate the cross sections by the parameter a. Generally, the cross section increases as a increases. If $a = 0$ then the cross section is zero hence the single look probability of no detection is equal to 1 implying that the single look probability of detection is equal to 0. This corresponds to observing the short side of a target.

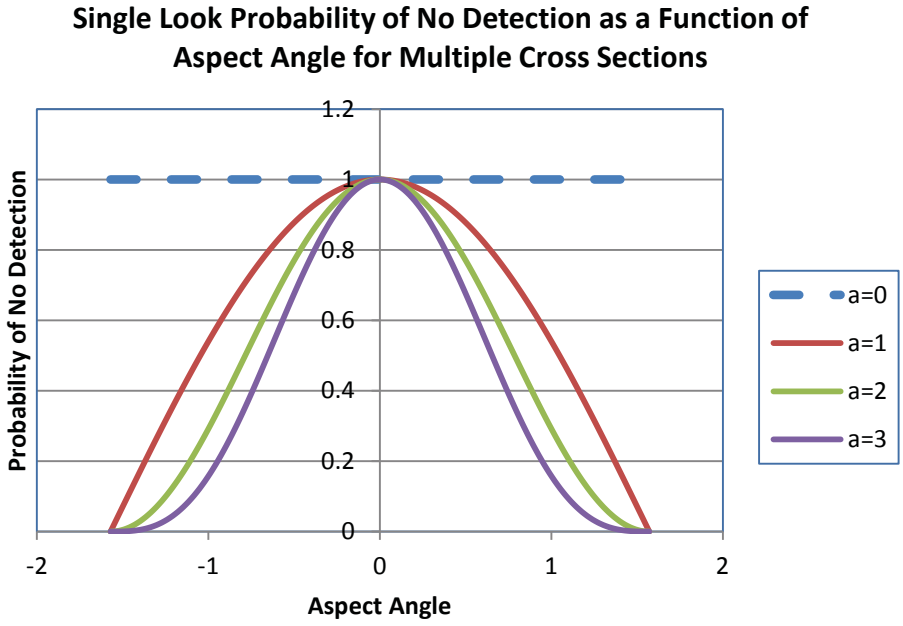

Figure 10: *Single look probability of no detection as a function of aspect angle for multiple cross sections.*

Example 7C. One look – tactics. In Figure 11, we plot the expected probabilities of detection as a function of SLRDP for multiple tactics based on one look. In the case of one look, a target is observed at one angle only. Hence, there is no optimization. Therefore, the first three tactics yield the same result. The last tactic (GBSL) gives a zero probability of detection since the searcher is guaranteed to observe the target at a zero GBSA. Note that, with one look, the expected probabilities of detection are substantially less than the aimed threshold of 0.95.

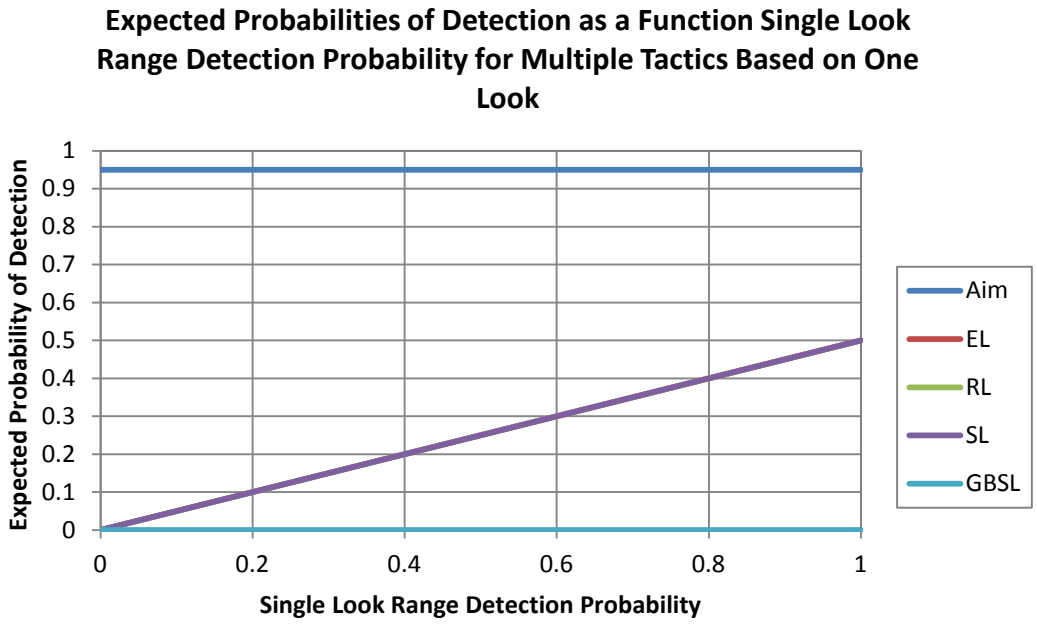

Figure 11: *Expected probabilities of detection as a function of SLRDP for multiple tactics based on one look.*

Example 7D. One look – cross sections. In Figure 12, we plot the expected maximal probabilities of detection as a function of SLRDP for multiple cross sections based on one look. It is shown that the expected maximal probabilities of detection increases with cross sections (increasing a). Note again that, with one look, the expected probabilities of detection are substantially less than the aimed threshold of 0.95.

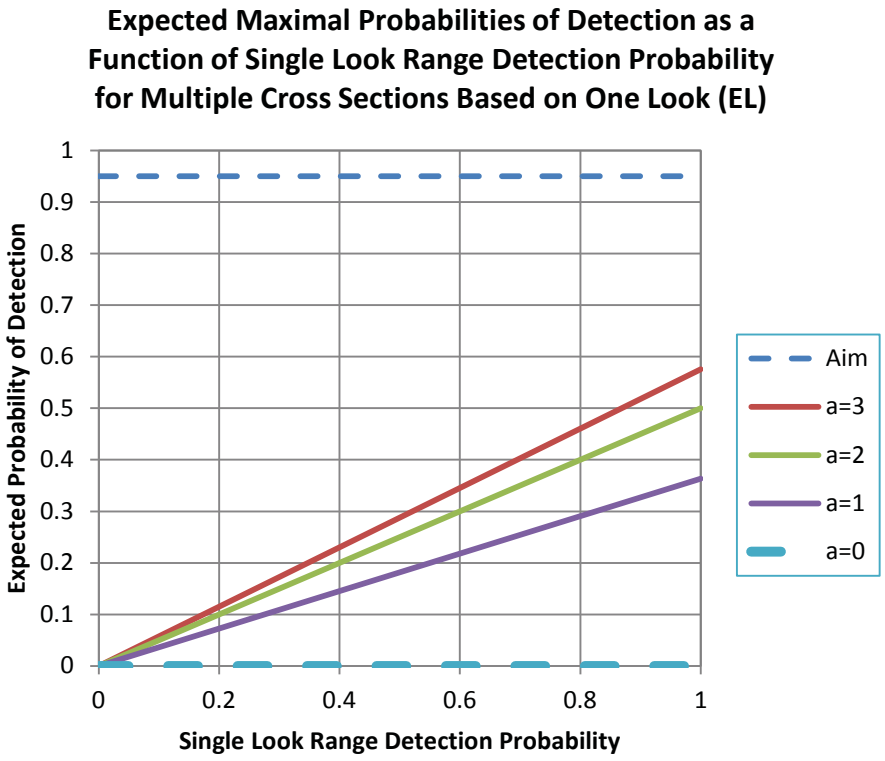

Figure 12: *Expected probabilities of detection as a function of SLRDP for multiple cross sections based on one look.*

Example 7E. Two looks – tactics. In Figure 13, we plot the expected probabilities of detection as a function of SLRDP for multiple tactics based on two looks. In the case of two looks, we can see the emerging differences in expected probabilities of detection. As anticipated, EL gives the highest expected probability of detection follow by RL, SL and GBSL in this order. Note that, with two looks, the expected probability of detection for maximal looks can be very close to the desired threshold of 0.95.

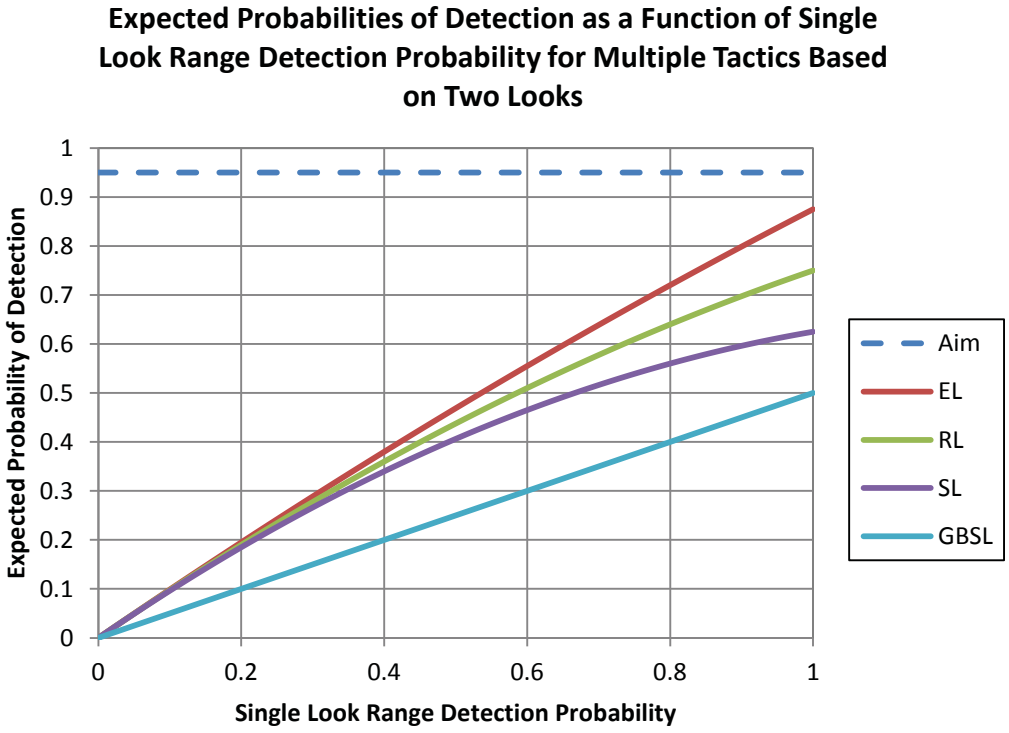

Figure 13: *Expected probabilities of detection as a function of SLRDP for multiple tactics based on two looks.*

Example 7F. Two looks – cross sections. In Figure 14, we plot the expected maximal probabilities of detection as a function of SLRDP for multiple cross sections based on two looks. It is shown that the expected maximal probabilities of detection increases with cross sections (increasing a). Note again that, with two looks and a substantial cross section, the expected probabilities of detection can be very close to the desired threshold of 0.95.

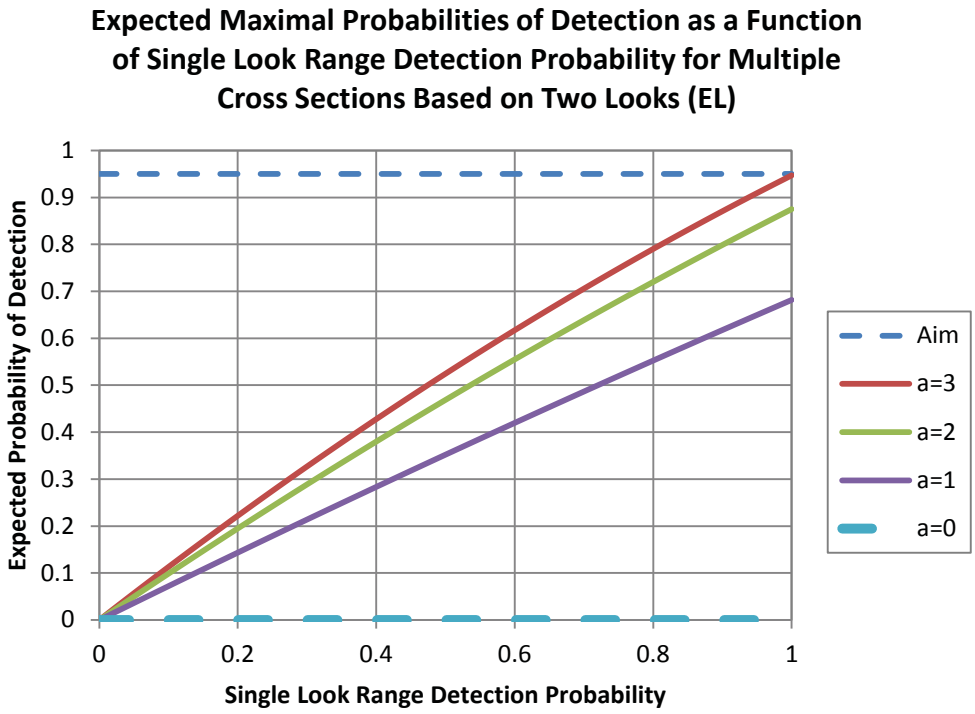

Figure 14: *Expected probabilities of detection as a function of SLRDP for multiple cross sections based on two look.*

Example 7G. Three looks – tactics. In Figure 15, we plot the expected probabilities of detection as a function of SLRDP for multiple tactics based on three looks. In the case of three looks, only EL can meet the threshold of 0.95. But RL can also be close to the threshold. At a high value of the SLRDP, GBSL is better than SL.

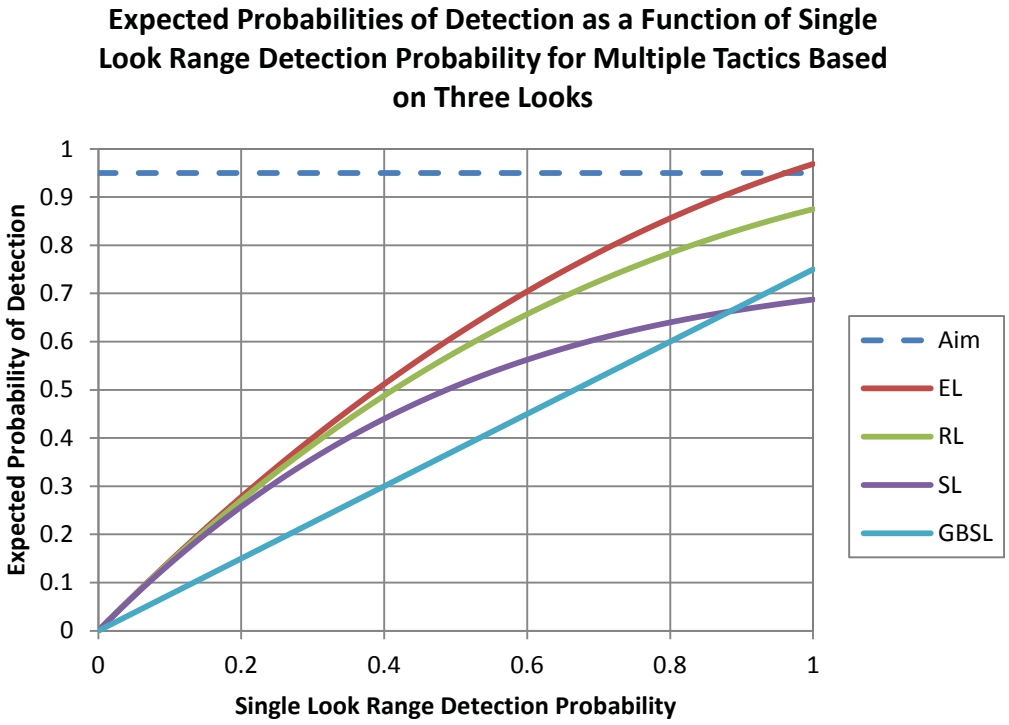

Figure 15: *Expected probabilities of detection as a function of SLRDP for multiple tactics based on three looks.*

Example 7H. Three EL looks – cross sections. In Figure 16, we plot the expected maximal probabilities of detection as a function of SLRDP for multiple cross sections based on three looks. It is shown that the expected maximal probabilities of detection increases with cross sections (increasing a). Note again that, with three looks and $a \geq 2$, the expected probabilities of detection can meet the threshold of 0.95.

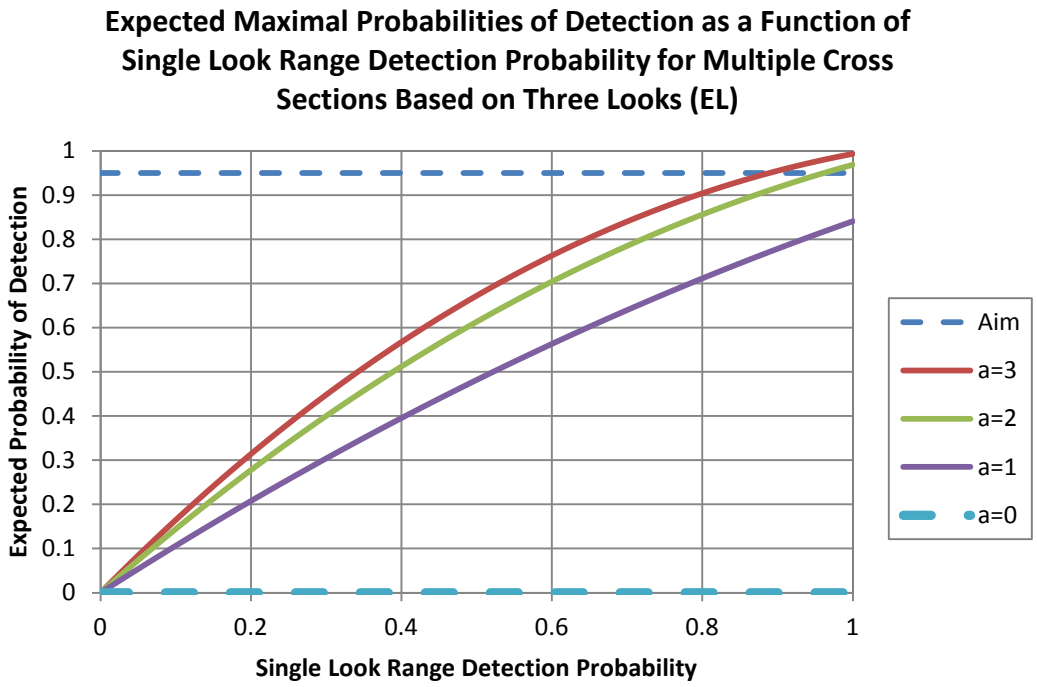

Figure 16: *Expected probabilities of detection as a function of SLRDP for multiple cross sections based on three looks.*

Example 7I. Four looks – tactics. In Figure 17, we plot the expected probabilities of detection as a function of SLRDP for multiple tactics based on four looks. In the case of four looks, EL and RL (almost) can meet the threshold of 0.95. At a high value of the SLRDP$\left(P \geq 0.8\right)$, GBSL is better than SL.

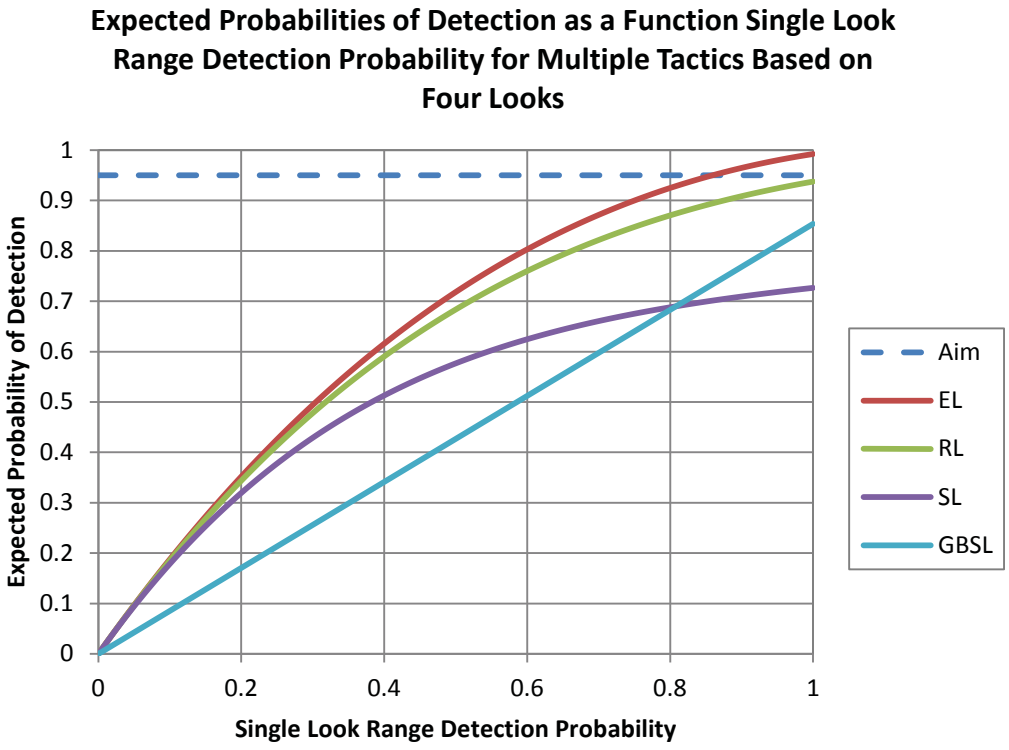

Figure 17: *Expected probabilities of detection as a function of SLRDP for multiple tactics based on four looks.*

Example 7J. Four EL looks – cross sections. In Figure 18, we plot the expected maximal probabilities of detection as a function of SLRDP for multiple cross sections based on four looks. It is shown that the expected maximal probabilities of detection increases with cross sections (increasing a). Note again that, with four looks and $a \geq 2$, the expected probabilities of detection can meet the threshold of 0.95. Even with $a = 1$, the expected maximal probability of detection is close to 0.95 for a high P.

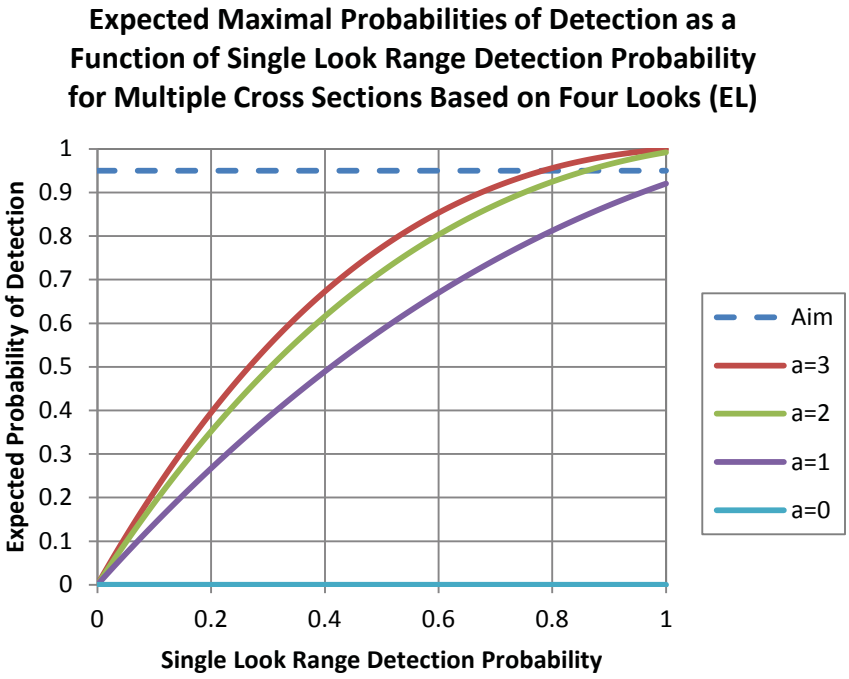

Figure 18: *Expected probabilities of detection as a function of SLRDP for multiple cross sections based on four looks.*

Example 7K. Five looks – tactics. In Figure 19, we plot the expected probabilities of detection as a function of SLRDP for multiple tactics based on five looks. In the case of five looks, the maximal looks and the random looks can meet the threshold of 0.95. The worst look can also be close to 0.95. At a high value of the SLRDP$\left(P \geq 0.8\right)$, GBSL is better than SL (repeating the same look angles).

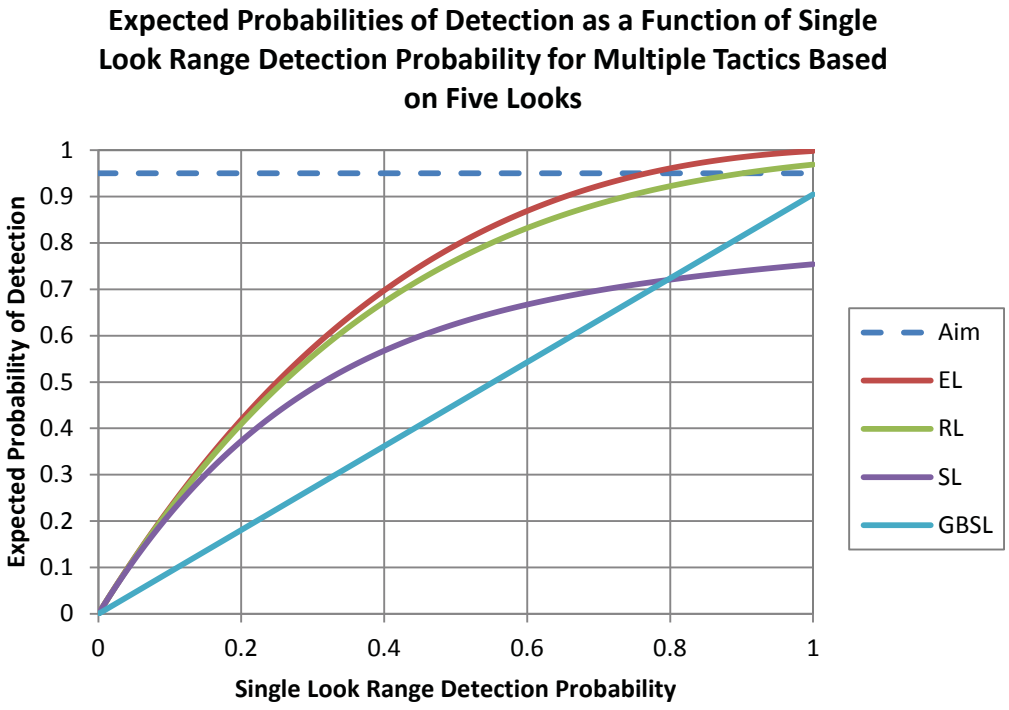

Figure 19: *Expected probabilities of detection as a function of SLRDP for multiple tactics based on five looks.*

Example 7L. Five EL looks – cross sections. In Figure 20, we plot the expected maximal probabilities of detection as a function of SLRDP for multiple cross sections based on five looks. It is shown that the expected maximal probabilities of detection increases with cross sections (increasing a). Note that, with five looks and $a \geq 1$, the expected probabilities of detection can meet the threshold of 0.95.

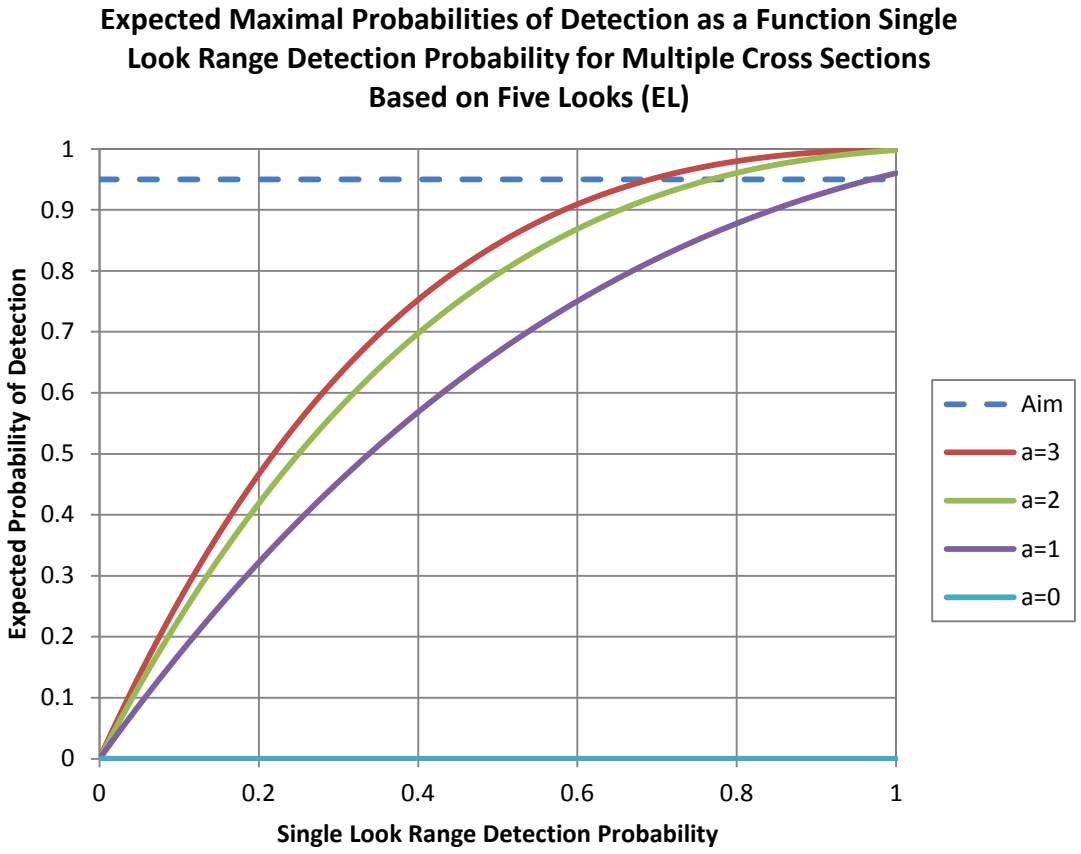

Figure 20: *Expected probabilities of detection as a function of SLRDP for multiple cross sections based on five looks.*

In this section, we have provided a sensitivity analysis on the expected probability of detection. We have shown that the expected probability of detection improves with the number of looks (n) and the cross section of the target (a) . What is more, the choices of tactics i.e., the look angles influence the expected probability of detection substantially.

8 Ellipsoidal mine

Mines have different shapes and usually have symmetry such as those of cylinder mines, spherical mines and Manta mines. Their shapes can be approximately modelled as an ellipsoid by varying the ellipsoid's parameters. Ref [19] provides the following parametrization of an ellipsoid:

$$x = A \cdot \cos u \cdot \cos v$$
$$y = B \cdot \cos u \cdot \sin v$$
$$z = C \cdot \sin u$$

where $u \in \left[-\frac{\pi}{2}, \frac{\pi}{2}\right]$ and $v \in [-\pi, \pi]$. Note that since A, B and C are not necessarily equal for a general ellipsoid and hence u and v are not necessarily the polar angle and the azimuth angle respectively. The dimensions of a mine are approximated from Ref [21]: $A = 1.60\ m; B = 0.325\ m\ and\ C = 0.325\ m$ as shown in Figure 21.

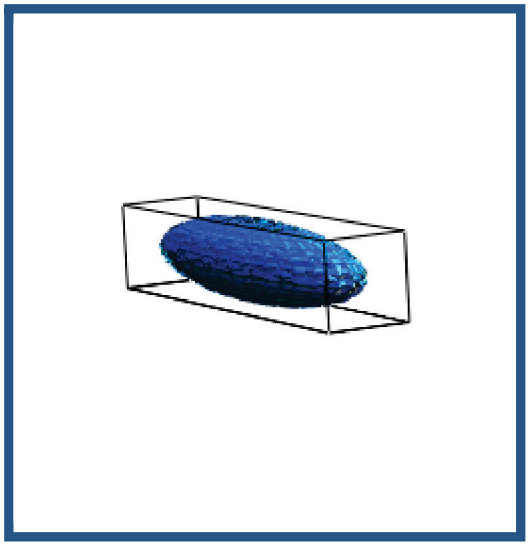

Figure 21: *A mine modelled as an ellipsoid.*

The cross section of an ellipsoid is the area resulting from the intersection of a plane that is perpendicular to the line of sight of the sensor with the ellipsoid. This plane must contain the centre of the ellipsoid. Since this intersection is an ellipse, its area can be written as:

$$\begin{aligned}\sigma_e &= \pi \cdot C \cdot \sqrt{A^2 \cdot \cos(\nu)^2 + B^2 \cdot \sin(\nu)^2} \\ &= \int z \cdot dr \\ &= 2 \cdot C \cdot \int_0^{\pi} du \cdot \sqrt{A^2 \cdot \cos(\nu)^2 + B^2 \cdot \sin(\nu)^2} \cdot \sin(u)^2\end{aligned}$$

where ν defines the orientation of the plane. Assuming that the probability of detection is maximal and is equal to one along the long axis of the ellipsoid, and is linear as a function of the cross section, we obtain:

$$\begin{aligned}f_e(\nu) &= \frac{\pi \cdot C}{\pi \cdot C \cdot A} \cdot \sqrt{A^2 \cdot \cos(\nu)^2 + B^2 \cdot \sin(\nu)^2} \\ &= \sqrt{\cos(\nu)^2 + \left(\frac{B}{A}\right)^2 \cdot \sin(\nu)^2}\end{aligned}$$

Alternately, the single look probability of no detection is given by:

$$g_e(\nu) = 1 - \sqrt{\cos(\nu)^2 + \left(\frac{B}{A}\right)^2 \cdot \sin(\nu)^2}$$

We plot g_e as a function of ν in Figure 22 as well as g_1 and g_2 where:

$$\begin{aligned}g_1(\nu) &= \lambda \cdot (1 - |\cos\nu|) \\ g_2(\nu) &= \lambda \cdot \left(1 - (\cos\nu)^2\right) \\ \lambda &= 0.8\end{aligned}$$

It is seen in Figure 22 that $g_1(\nu) \le g_e(\nu) \le g_2(\nu)$. The difference between the expressions for g between Section 7 and Section 8 is that in the former the minimal probability corresponding to the short side of a target is zero while in the latter that probability is non zero. By modifying the function g, we can bound the probability of no detection for an ellipsoid between $a = 1$ and

$a = 2$. This gives us the confidence that we can model the cross section using the parameter a.

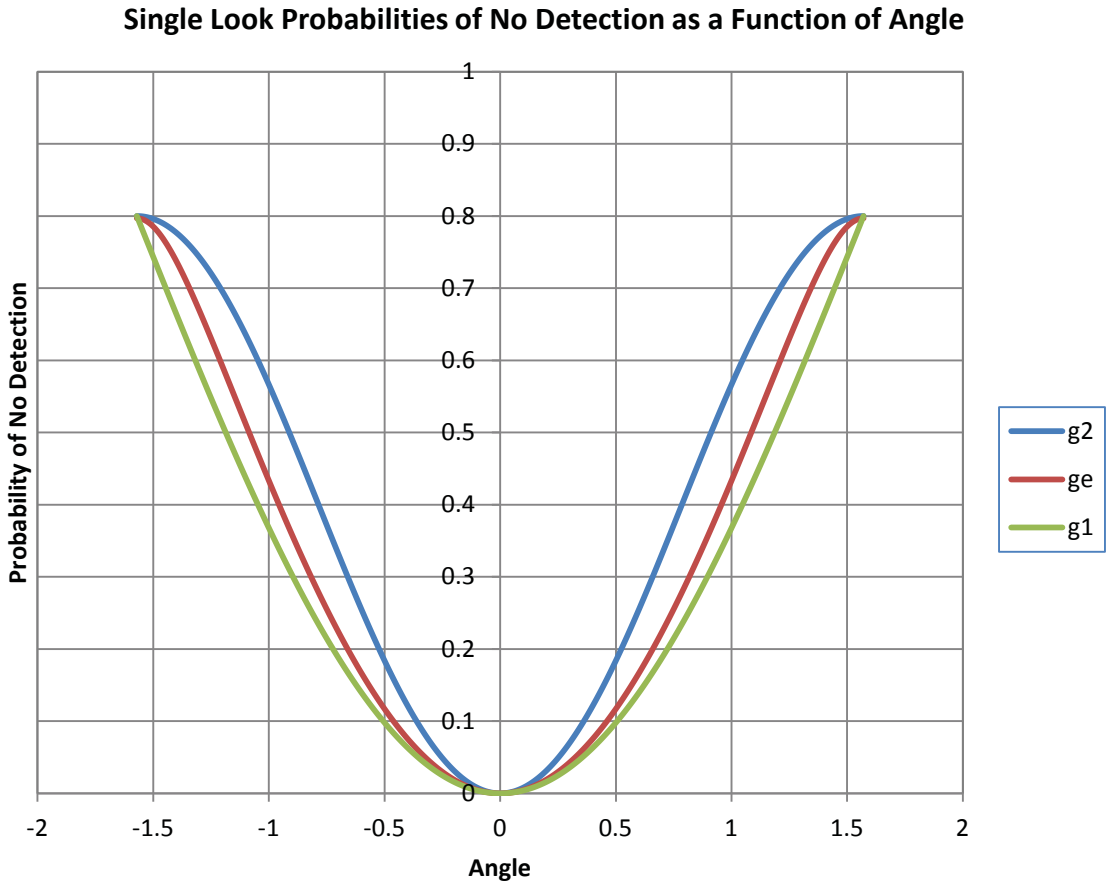

Figure 22: *Single look probabilities of no detection as a function of angle* ν .

We plot the expected maximal probabilities of detection as a function of SLRDP for one look up to five looks (EL) in Figure 23. Comparing Figure 23 to Figure 12, Figure 14, Figure 16, Figure 18, Figure 20, we see a significant improvement in the expected maximal probability of detection. This is due to the non-zero minimal cross section of an ellipsoid which of course corresponds to a non-zero minimal probability of detection for single looks. For example, with a zero minimal probability of detection in Section 7, it takes at least three looks to achieve the threshold of 0.95 for $1 \le a \le 2$ while with a non-zero minimal probability of detection in this section, it requires only two looks to achieve the same threshold. Also, the requirement of the SLRDP to achieve this threshold is less stringent in the case of non-zero minimal cross section. For instance, with three looks, the minimal SLRDP is approximately 0.84 for non zero minimal cross section while it is approximately 0.97 for zero minimal cross section (with $a = 2$).

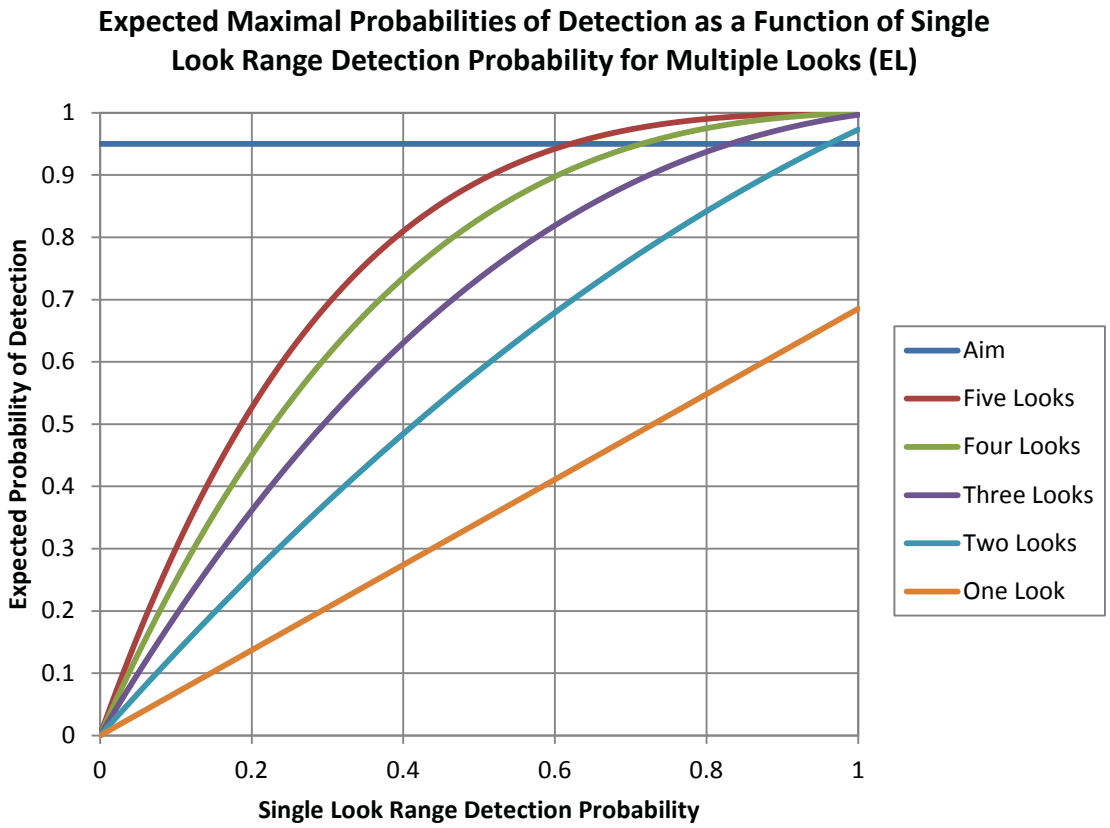

Figure 23: *Expected maximal probabilities of no detection as a function of SLRDP for multiple looks.*

9 Discussion

In Section 7, we provide numerical results, based on a simplified model of a mine, for a number of metrics related to the probability of detection. It is shown clearly that the expected maximal probability of detection improves significantly with the number of looks. The improvement is substantial for few looks e.g., the two look case can yield an expected maximal probability of detection that is almost twice of the one given by the one look case. This validates the benefits of multiple looks.

We examine four tactics: the maximal looks, the random looks, the same looks and the guaranteed broad side look. They are defined in Section 7. It is known, Ref [15], that by choosing the appropriate characteristic of the search patterns such as the spacing between two consecutive parallel tracks, we can set the SLRDP to be greater than or equal to $P \geq 0.9$. Therefore, the discussion below is made assuming this condition.

The maximal looks provide the best expected probability of detection since it was shown to be a globally maximal tactic in Ref [16]. This tactic is simple, robust and easy to implement. An example of this implementation with three looks is called the star pattern, Refs [22][23].

The random looks provide the second best expected probability of detection. By choosing each look angle in a uniformly independent and random way, there is a high chance that the look angles are similar to the maximal angles. This is so as the maximal angles are distributed uniformly (in a discrete way) i.e., $\mu_i = i \cdot \frac{\pi}{n}$ where μ_i is the ith look with $i = 0,...,n-1$. Their similarities with the maximal looks make the corresponding expected probabilities of detection close to those given by the maximal looks. The Koopman's random search tactic would simulate such random looks.

The same looks observe a target at the same aspect angle multiple times. There is a high chance that the target is observed at a single look low probability of detection angle since the orientation of the target is uniformly random. This means that as the number of looks increases, the effectiveness of the same looks decrease. This is generally the worst tactic for search and detection. An implementation of this tactic would be carried out by repeating a same search pattern such as the parallel tracks multiple times.

GBSL is the best look in the worst case. As the number of looks increases, the chance of observing a target on its broad side increases. Hence, GBSL can be better than the same look case for multiple looks. We see that very clearly for four looks and five looks. The look can be obtained by implementing the maximal look tactic such as the parallel tracks or the star search patterns. GBSL is a conservative tactic in the sense that with one scan of the area by the parallel tracks for example, we are guaranteed that in the worst case a target is observed at GBSA or better. This means that we do not need to repeat the experiment many times to get GBSL result unlike the three other tactics described above that are expected values averaging over all possible aspect angles.

In addition to the analysis of tactics based on multiple look effects, we also analyze the effects of the cross sections. The cross section of a target is simulated by the parameter a which increases with increasing cross sections. By the definition of a, the cross section is zero when $a = 0$. This corresponds to observing a cylindrical target on its short side. Although, in this TM, we model a as a constant parameter, all the results can be extended to the case where a is a function of the aspect angle (θ) as long as it has the same characteristics of $g(\theta)$. That is, $a = a(\theta)$ with:

$$\frac{\partial a}{\partial \theta} \geq 0 \quad \theta \in \left[0, \frac{\pi}{2}\right]$$
$$\frac{\partial a}{\partial \theta} \leq 0 \quad \theta \in \left[-\frac{\pi}{2}, 0\right]$$
$$a(\theta) = a(-\theta)$$
$$a(\theta + \pi) = a(\theta)$$

Such a generalization will be useful if we fit $g(\theta)$ to simulate the shape of a known target. Furthermore, we investigate the effects of a non-zero minimal cross section which is the case for a real target. To do this, we model a target as an ellipsoid and found that the expected maximal probability of detection increases substantially. We can theoretically achieve an 0.95 expected maximal probability of detection with three looks for the ellipsoid model while we would need three looks to achieve the same threshold with a zero minimal cross section.

10 Conclusion

In this paper, the angular dependence of the detection process which is often overlooked for search and detection missions is explicitly accounted for by assuming that the target possesses rectangular symmetry. As a consequence of this approximate symmetry, the broad side of a target is endowed with the largest cross section, which results in the highest probability of detection given that the target is observed only once. However, since the orientation of the target is in general unknown, there is likelihood that it will be imaged on the short side, i.e., the smallest cross-section. Therefore, the probability of detecting the target may not be one hundred percent even if the search area is entirely covered. Making several observations of the target in order to increase the change of observing its broad side is one way to address this problem.

We show that EL (equidistant looks) provides the best probability of detection followed by RL (random looks). GBSL (guaranteed broad side look) is comparable to SL (same looks). Generally, as the number of looks increases and for sufficiently large range detection probability GBSL provides a better probability of detection than the one from SL.

In this TM, we have shown how to determine two characteristic metrics related to the probability of detecting a target. That is, the expected probability of detection and the guaranteed broad side look. The methodology is simple and can be implemented easily in a symbolic computational software such as MathCad Version 14, Ref [24]. We have shown the effects of multiple looks, tactics, cross sections and non-zero minimal cross sections. It is our hope that these results will eventually be incorporated into the search and detection manual of the CAF as they will improve the planning and the effectiveness of a search and detection mission.

In the future, if circumstances permit, we plan to implement these results into an existing simulation named MISO (Mine Inspection & Search Operations, Refs [22][25]) that was initially developed at DRDC Atlantic and was recently upgraded at DRDC CORA under the Technology Investment Fund (TIF) project 10bz04 on emerging behaviours for multiple autonomous agents awarded for 2013-2013.

This page intentionally left blank.

References

[1] Zerr B., Bovio, E. and Stage, B. (2001), Automatic Mine Classification Approach Based on AUV Manoeuvrability and COTS Side Scan Sonar, In *Proceedings of the Autonomous Underwater Vehicle and Ocean Modelling Networks: GOAT2 2000 Conference*, CP-46, 315-322, NATO Saclant Undersea Research Centre, La Spezia, Italy.

[2] Fawcett, J. A., Crawford, A., Hopkin, D., Myers, V., Couillard, M., and Zerr, B. (2008), Multi-Aspect Computer-Aided Classification of the Citadel Trial Side-Scan Sonar Images (U), (DRDC Atlantic TM 2008-029), Defence R&D Canada – Atlantic.

[3] Runkle P., Bharadwa, P. K., Couchman, L., and Carin, L. (1999), Hidden Markov Models for Multiaspect Target Classification, *IEEE Transactions on Signal Processing*, 47(7), 2035-2040.

[4] Robinson, M., Azimi-Sadjadi, M. R., and Salazar, J. (2005), Multi-Aspect Target Discrimination Using Hidden Markov Models and Neural Networks, *IEEE Transactions on Neural Networks*, 16(2), 447-459.

[5] Shihao, J. and Xuejun, L. (2005), Adaptive Multiaspect Target Classification and Detection with Hidden Markov Models, *IEEE Sensors Journal*, 5(5), 1035-1042.

[6] Martínez, S. and Bullo, F. (2006), Optimal Sensor Placement and Motion Coordination for Target Tracking, *Automatica*, 42(4), 661-668.

[7] Ash, J. N. and Moses, R. L. (2008), On Optimal Anchor Node Placement in Sensor Localization by Optimization of Subspace Principal Angles, In *Proceedings of IEEE International Conference on Acoustics, Speech, and Signal Processing*, 2289-2292, Las Vegas, USA.

[8] Bishop, A. N. and Jemsfelt P. (2009), An Optimality Analysis of Sensor-Target Geometries for Signal Strength Based Lozalization, In *Proceedings of the 5th International Conference on Intelligent Sensors, Sensor Networks and Information Processing (ISSNIP'09)*, 127-132, Melbourne, Australia.

[9] Bishop, A. N., Fidan, B., Anderson, B. D. O., Doğançay, K., and Pathirana, P. N. (2010), Optimality Analysis of Sensor-Target Localization Geometries, *Automatica*, 46(3), 479-492.

[10] Koopman B. O. (1980), Law of Random Search, In *Search and Screening: General Principles with Historical Applications*, New York : Pergamon Press, p. 71-74.

[11] Nguyen, B. U., Hopkin, D, and Yip, Handson. Autonomous Underwater Vehicles – A Transformation of Mine Counter Measure Operations, Defense & Security Analysis, Vol 24 No 3, Sep 08, 20 pages.

[12] Bourque, A. and Bao Nguyen. Optimal sensor configuration cylindrical target detection. 9th IEEE international conference on control and automation, 19-22 Dec 11, Santiago, Chile, 6 pages.

[13] Nguyen, B. U., Hopkin D. and Yip H. Autonomous underwater vehicles conducting mine countermeasure operations, DRDC CORA TM 2008-42, Oct 08, 54 pages.

[14] Nguyen, B. U. and David Hopkin. Concepts of operations for the side scan sonar Autonomous Underwater Vehicles developed at DRDC Atlantic, DRDC Atlantic TM 2005–213 Nov 05, 70 pages.

[15] Nguyen, B. and Hopkin, D. (2005), Modeling Autonomous Underwater Vehicle (AUV) Operations in Mine Hunting, In *Proceedings of Oceans 2005 – Europe Conference*, 533-538, Brest, France.

[16] Nguyen, B. U. and Alex Bourque. A robust & globally optimal search tactic for targets exhibiting mirror symmetry, draft Dec 11, 68 pages.

[17] Gradshteyn, I. S. and Ryzhik, I. M. (1979), Table of Integrals, Series, and Products, 4th ed. San Diego: Academic Press, p. 34.

[18] Gradshteyn, I. S. and Ryzhik, I. M. (1979), Table of Integrals, Series, and Products, 4th ed. San Diego: Academic Press, p. 33.

[19] Gradshteyn, I. S. and Ryzhik, I. M. (1979), Table of Integrals, Series, and Products, 4th ed. San Diego: Academic Press, p. 369.

[20] http://en.wikipedia.org/wiki/Ellipsoid. Last accessed August 15, 2014.

[21] Wille, Peter. Sound images of the ocean in research and monitoring, vol 1, Springer-Verlag Berlin Heidelberg, 2005, p. 365.

[22] Li, Guichong and Bao Nguyen A simulation for autonomous underwater vehicles in a multiple mine environment, draft Dec 11, 50 pages.

[23] Nguyen, B. U., Matthew Bays, Apoorva Shende and Daniel Stilwell. An approach to subsea survey for safe naval transit. Oceans 2011 Conference, 19-22 Sep 11, Maui (IEEE proceedings), 6 pages.

[24] MathCad 14.0, Parametric Technology Corporation, 07.

[25] MacDonald Dettwiler Associates, Upgrading Mine Hunting Software, Jun 06. P. Zhang and David Morash, Mine Inspections and Search Operations, Contract Report, Jun 06.

List of symbols/abbreviations/acronyms/initialisms

CAF	Canadian Forces
CORA	Centre for Operational Research and Analysis
DND	Department of National Defence
DRDC	Defence Research & Development Canada
DRDKIM	Director Research and Development Knowledge and Information Management
EL	Equidistant looks
GBSA	Guaranteed Broad Side Angle
GBSL	Guaranteed Broad Side Look
MCM	Mine Counter Measures
MISO	Mine Inspection and Search Operations
QED	Quod Erat Demonstrandum
R&D	Research & Development
RL	Random looks
SL	Same (repeated) looks
SLRDP	Single Look Range Detection Probability
TIF	Technology Investment Fund
TM	Technical Memorandum

(x,y,z)	Cartesian coordinate system
f_e	Probability of detection of a single look based on the cross section of an ellipsoid
$\hat{v}$	Guaranteed Broad Side Angle
v_{max}	Best angle of observation
$\delta_{i,j}$	Kronecker delta
$\hat{\theta}$	Orientation angle of a target when $\nu = \hat{\nu}$
σ_e	Cross section of an ellipsoid
B	Half the length of an ellipsoid
$B(,)$	Beta function
dx	Integration variable

G( )	Expected probability of not detecting a target based on multiple looks
gcd	Greatest common divisor
k	Summing index
P_e	Expected probability of detection
q	m divided by the greatest common divisor of m and n
r	n divided by the greatest common divisor of m and n
V_i	Angle of observation for the ith look
$\Gamma( )$	Gamma function
A	Half the width of an ellipsoid
C	Half the height of an ellipsoid
I	Integrand of the expected probability of no detection
P, P_r	Probability of detection due to range
Q, Q_r	Probability of no detection due to range
a	Parameter simulating the cross section of a target
$g(x)$	Probability of detection as a function of angle x for a single look
i	Counter
m	Counter
n	Counter or number of looks
p	Greatest common divisor of m and n
u	Angular parameter defining the surface of an ellipsoid
v	Angular parameter defining the surface of an ellipsoid
x	Angle and direction // MULTIPLE USES
θ	Angle
λ	Parameter defining the probability of no detection
μ	Look angle
ϕ	$1 + 2\ Q\ /\ P$

DOCUMENT CONTROL DATA

(Security markings for the title, abstract and indexing annotation must be entered when the document is Classified or Designated)

1. ORIGINATOR (The name and address of the organization preparing the document. Organizations for whom the document was prepared, e.g., Centre sponsoring a contractor's report, or tasking agency, are entered in Section 8.)

Defence Research and Development Canada – CORA
101 Colonel By Drive
Ottawa, Ontario K1A 0K2

2a. SECURITY MARKING (Overall security marking of the document including special supplemental markings if applicable.)

UNCLASSIFIED

2b. CONTROLLED GOODS

(NON-CONTROLLED GOODS)
DMC A
REVIEW: GCEC DECEMBER 2012

3. TITLE (The complete document title as indicated on the title page. Its classification should be indicated by the appropriate abbreviation (S, C or U) in parentheses after the title.)

Modelling metrics for mine counter measure operations

4. AUTHORS (last name, followed by initials – ranks, titles, etc., not to be used)

Nguyen, B.; Mirshak, R.

5. DATE OF PUBLICATION (Month and year of publication of document.)

August 2014

6a. NO. OF PAGES (Total containing information, including Annexes, Appendices, etc.)

58

6b. NO. OF REFS (Total cited in document.)

25

7. DESCRIPTIVE NOTES (The category of the document, e.g., technical report, technical note or memorandum. If appropriate, enter the type of report, e.g., interim, progress, summary, annual or final. Give the inclusive dates when a specific reporting period is covered.)

Scientific Report

8. SPONSORING ACTIVITY (The name of the department project office or laboratory sponsoring the research and development – include address.)

Defence Research and Development Canada – CORA
101 Colonel By Drive
Ottawa, Ontario K1A 0K2

9a. PROJECT OR GRANT NO. (If appropriate, the applicable research and development project or grant number under which the document was written. Please specify whether project or grant.)

TIF 10bz04

9b. CONTRACT NO. (If appropriate, the applicable number under which the document was written.)

10a. ORIGINATOR'S DOCUMENT NUMBER (The official document number by which the document is identified by the originating activity. This number must be unique to this document.)

DRDC-RDDC-2014-R58

10b. OTHER DOCUMENT NO(s). (Any other numbers which may be assigned this document either by the originator or by the sponsor.)

11. DOCUMENT AVAILABILITY (Any limitations on further dissemination of the document, other than those imposed by security classification.)

Unlimited

12. DOCUMENT ANNOUNCEMENT (Any limitation to the bibliographic announcement of this document. This will normally correspond to the Document Availability (11). However, where further distribution (beyond the audience specified in (11) is possible, a wider announcement audience may be selected.))

Unlimited

13. ABSTRACT (A brief and factual summary of the document. It may also appear elsewhere in the body of the document itself. It is highly desirable that the abstract of classified documents be unclassified. Each paragraph of the abstract shall begin with an indication of the security classification of the information in the paragraph (unless the document itself is unclassified) represented as (S), (C), (R), or (U). It is not necessary to include here abstracts in both official languages unless the text is bilingual.)

In this scientific report, we present a methodology to determine the expected probabilities of detection of a target based on multiple looks at that target. We provide a sensitivity analysis of the probabilities of detection based on the number of looks, tactics and cross sections. Generally, the probability of detection improves significantly with the number of looks. Its value can vary substantially with the search and detection tactics as well as the cross section of a target. There are three tactics identified here where each look is independent of the others. The first tactic is a globally optimal tactic where the consecutive look angles are equidistant. The second tactic distributes the look angles randomly. The third tactic imposes the same angle for all look angles. In addition, we extract the guaranteed best angle of the broad side of a target from the first tactic. For each tactic, we propose an example of a corresponding search pattern. The methodology in this report can be implemented easily on any computational symbolic software; MathCad version 14 was used herein. We hope to make the search and detection community aware of the phenomenologies of multiple looks, and hope that the material presented will be incorporated into the mine search and detection tactics of the CAF.

Dans le présent rapport scientifique, nous exposons une méthodologie pour déterminer les probabilités attendues de détection d'une cible en multivisée. Nous exposons une analyse de sensibilité des probabilités de détection fondées sur le nombre de visées, les tactiques et les sections efficaces radar . De façon générale, la probabilité de détection augmente de façon importante avec le nombre de visées. Sa valeur peut varier considérablement en fonction des tactiques de recherche et de détection et de la section efficace radar. Nous présentons ici trois tactiques dans lesquelles chaque visée est indépendante des autres. La première est une tactique optimale globale dans laquelle les angles de visée consécutifs sont équidistants. Dans la deuxième tactique, les angles de visée sont répartis aléatoirement. Quant à la troisième tactique, tous les angles de visée sont identiques. En outre, la première tactique nous permet de déduire le meilleur angle garanti du flanc d'une cible. Pour chaque tactique, nous proposons un exemple du circuit de recherche correspondant. La méthodologie présentée dans le rapport peut être mise en œuvre facilement à l'aide de n'importe quel logiciel de calcul symbolique; de notre côté, nous avons utilisé la version 14 de MathCad. Nous souhaitons sensibiliser la communauté de la recherche et de la détection aux phénomènes des visées multiples, et nous espérons que le matériel présenté sera intégré aux tactiques de recherche et de détection des mines des FAC.

14. KEYWORDS, DESCRIPTORS or IDENTIFIERS (Technically meaningful terms or short phrases that characterize a document and could be helpful in cataloguing the document. They should be selected so that no security classification is required. Identifiers, such as equipment model designation, trade name, military project code name, geographic location may also be included. If possible keywords should be selected from a published thesaurus, e.g., Thesaurus of Engineering and Scientific Terms (TEST) and that thesaurus identified. If it is not possible to select indexing terms which are Unclassified, the classification of each should be indicated as with the title.)

Optimization, Symmetry, Multi-Aspect, Search Strategy, Detection, Mine Hunting, Sensor Network, Data fusion, Mines, metrics, search tactics